Vol. 586: 91–112, 2018
https://doi.org/10.3354/meps12367

MARINE ECOLOGY PROGRESS SERIES
Mar Ecol Prog Ser

Published January 11

Distribution of *Phaeocystis antarctica*-dominated sea ice algal communities and their potential to seed phytoplankton across the western Antarctic Peninsula in spring

Virginia Selz[1,*], Kate E. Lowry[1], Kate M. Lewis[1], Hannah L. Joy-Warren[1], Willem van de Poll[2], Sandip Nirmel[1], Amy Tong[1], Kevin R. Arrigo[1]

[1]Department of Earth System Science, Stanford University, Stanford, CA 94305, USA
[2]Department of Ocean Ecosystems, Energy and Sustainability Research Institute Groningen, University of Groningen, Nijenborgh 7, 9747 AG Groningen, The Netherlands

ABSTRACT: The western Antarctic Peninsula has experienced extreme changes in the timing of sea ice melt and freeze up, shortening the duration of the seasonal sea ice cycle. While previous research demonstrated connections between multiple pelagic trophic levels and the physics of the sea ice, few studies have assessed the sea ice ecosystem or its linkage to the ocean ecosystem in this region. Through a field survey and shipboard experiments, our study focused on characterizing the spring ice algal bloom and elucidating its role in seeding phytoplankton communities post-ice melt in high and low light conditions. Field data revealed that algal communities in slush layers, often formed from the flooding of seawater (infiltration layers), dominated biomass distributions in the sea ice throughout the region, and showed distinct photophysiological characteristics from interior or bottom ice communities. Sea ice algal biomass reached 120 mg chl *a* m^{-2} and was often dominated by *Phaeocystis antarctica.* Shipboard growth experiments showed that prior light history (ice or water column), rather than community composition (phytoplankton and ice algae were composed of similar taxa), primarily drove physiological responses to high and low light. *P. antarctica* generally dominated the community in growth experiments at the end of the 6 d incubation period. Settling column experiments suggested that *P. antarctica*'s higher sinking rates relative to other taxa may explain its minor contributions to the summer phytoplankton community in single-cell form and its absence in colonial form, observed in the long-term ecological record of this region.

KEY WORDS: Photophysiology · Diatoms · Ice–ocean coupling · Community composition

INTRODUCTION

Sea ice harbors a rich microbial community composed of bacteria, algae, and zooplankton that is critical in fueling upper trophic levels in early spring (Ackley & Sullivan 1994), yet there is a paucity of field data on ice algal blooms in Antarctic sea ice (Meiners et al. 2012). Even less is understood about the fate of ice algae following ice melt, and their potential role in seeding the water column and impacting phytoplankton bloom development. Ice algal blooms contribute approximately 10 to 28% of annual primary production in ice-covered regions across the Southern Ocean (Arrigo & Thomas 2004), and sea ice often contains bloom-forming phytoplankton taxa such as diatoms and *Phaeocystis antarctica* (Garrison et al. 1987, Mangoni et. al 2009, Lannuzel et al. 2013). Beyond the role ice algae play

*Corresponding author: vselz@stanford.edu

in initiating spring production in the ice and potentially in the water column (Ackley & Sullivan 1994), they also contribute to biogeochemical cycling of carbon and sulfur through their production of organic carbon and dimethylsulfoniopropionate, respectively (Tison et al. 2010, Vancoppenolle et al. 2013). Understanding the coupling between the ice and ocean ecosystem is thus critical, especially in regions with rapidly changing ice conditions, such as the western Antarctic Peninsula (WAP).

The WAP and surrounding seas have experienced rapid and intense warming over the last 50 yr (Marshall et al. 2002, Vaughan et al. 2003, Meredith & King 2005, Turner et al. 2005). Increasing spring and winter surface temperatures have been accompanied by declines in sea ice concentration and duration (Stammerjohn et al. 2008). The changing properties of sea ice, including thinning and greater lead fractions (Liu et al. 2004, Stammerjohn et al. 2008), and increasingly warm northerly winds (Massom et al. 2006) promote earlier spring melt. Warm northerly winds also contribute to delayed freeze up and limit the northward advance of sea ice (Stammerjohn et al. 2008). These ice–atmosphere interactions modify ice dynamics along the WAP and are sensitive to large-scale atmospheric variability, including the Southern Annular Mode and the El Niño–Southern Oscillation (Massom et al. 2006, Stammerjohn et al. 2008).

Changes in WAP sea ice dynamics have affected primary producers on regional scales. Across the WAP, both satellite records spanning 3 decades (Montes-Hugo et al. 2009) and long-term field studies suggest that phytoplankton bloom magnitude (Vernet et al. 2008, Annett et al. 2010, Venables et al. 2013, Rozema et al. 2017), size structure, and community composition (Montes-Hugo et al. 2008) are driven by ice-influenced resource availability (light and nutrients). Large-scale atmosphere–ice–ocean interactions affect the stratification of the water column (Massom & Stammerjohn 2010) and the intrusion and upwelling of nutrient-rich upper Circumpolar Deep Water to the surface ocean (Martinson et al. 2008). These atmosphere–ice–ocean dynamics affect the availability of light and nutrients to phytoplankton and have been linked to large-scale changes in primary productivity along a north–south gradient (Montes-Hugo et al. 2009, Venables et al. 2013). Between 1979 and 2004, the northern section of the WAP (as defined by Montes-Hugo et al. 2009) transitioned from a seasonally ice-covered to a nearly ice-free region. This decreased ice cover led to enhanced wind-driven mixing and reduced light availability (Montes-Hugo et al. 2009, Ducklow et al. 2013, Steinberg et al. 2015). These physical changes corresponded to an 89% reduction in surface summer phytoplankton chlorophyll *a* (chl *a*) over a 30 yr period (Montes-Hugo et al. 2009) and a predominance of small phytoplankton, such as cryptophytes (Montes-Hugo et al. 2008). In contrast, in the southern WAP, shifts from perennial to seasonal ice have maintained ice-melt-induced stratification in spring, increasing light availability in recent years (Montes-Hugo et al. 2009). These favorable growth conditions in the southern WAP were linked to a 66% increase in surface chl *a* over a 30 yr period (Montes-Hugo et al. 2009) and a predominance of large diatoms (Montes-Hugo et al. 2008).

In addition to the phytoplankton community, decadal surveys have linked the abundance of secondary producers to ice conditions, with the 2 dominant grazers — krill and salps — following opposing trends (Ross et al. 2008, 2014, Steinberg et al. 2015). While the abundance of some krill species corresponded to high ice conditions, increased salp abundance coincided with low ice conditions (Ross et al. 2008, 2014, Steinberg et al. 2015). Other studies have observed shifts from krill to salp dominance with decreasing sea ice on shorter timescales (Loeb et al. 1997, Ducklow et al. 2007), particularly in the northern WAP (Bernard et al. 2012). The strong linkage of krill populations to sea ice dynamics is likely driven by the necessary role that sea ice plays as a refuge (Daly & Macaulay 1988) and food source for juvenile krill (Kottmeier et al. 1987, Marschall 1988, Daly 1990).

The Antarctic ice pack acts as a habitat for multiple trophic levels that are supported by ice algal communities found at the surface, interior, or bottom of the ice (Arrigo & Thomas 2004), depending on its physical structure. During late winter and early spring, snow loading often depresses the surface of the ice below sea level, resulting in surface flooding, melting snow, and seawater percolating through the ice (Perovich et al. 2004). Variations in salinity and temperature lead to freezing point differentials throughout the vertical profile of the sea ice, creating a 'honeycomb-like ice matrix filled with sea water below a surface layer of snow and ice' (Ackley & Sullivan 1994, p. 1, Ackley et al. 2008), or slush layers. These slush layers — also known as gap (Ackley & Sullivan 1994, Jeffries et al. 1997) or infiltration layers — can support high concentrations of algal biomass (172 to 370 mg chl *a* m^{-3}; Fritsen et al. 1998, 2001, Kattner et al. 2004), potentially due to their porous nature and enhanced seawater exchange (Massom et al. 2006). Flooding occurs over approximately 15 to 30% of the ice pack in Antarctica (Wadhams et al. 1987) and up

to 50% of the ice area along the WAP (Saenz & Arrigo 2014), especially in late winter and early spring (Perovich et al. 2004). Because of this enhanced flooding, Perovich et al. (2004) suggested that sea ice in the WAP experiences an extended spring from August to December and further indicated that these widespread porous layers may be more accessible to juvenile krill along the WAP than elsewhere in the Antarctic sea ice.

Along the WAP, physical mechanisms, such as flushing of melt water through brine channels or infiltration of surface waves (Thomas et al. 1998), and the mechanical break up of ice expel the slush and ice algae into the water column and create an ice slurry at the surface (Massom et al. 2006). During this early spring period, ice-derived phytoplankton can potentially serve as a seed population in the water column (Massom et al. 2006). However, despite the potential ecological significance of ice algae in early spring (Ackley & Sullivan 1994) to both upper trophic levels (Perovich et al. 2004) and primary production (Massom et al. 2006), to date few field studies have investigated ice biology and its potential linkages to the water column along the WAP. Using field survey data, our study characterized the spring sea ice algal bloom along the WAP, significantly advancing our knowledge of the biomass, physiology, and species composition of sea ice communities in mid to late spring. In addition, we used controlled experiments to focus on the potential for ice algal communities to seed phytoplankton communities under different light conditions in the water column. Together our results show the extent to which sea ice algal communities contribute to pelagic primary production after melting out of the sea ice along the WAP. To our knowledge, this is the first dataset of these measurements taken along the Palmer Long Term Ecological Research grid (PAL-LTER) in spring (November).

MATERIALS AND METHODS

Field data collection

Samples were collected from the RVIB 'Nathaniel B. Palmer' along the extended PAL-LTER grid of the WAP (Fig. 1, Table 1) during the *Phaeocystis antarctica* Adaptive Responses in the Antarctic Ecosystem

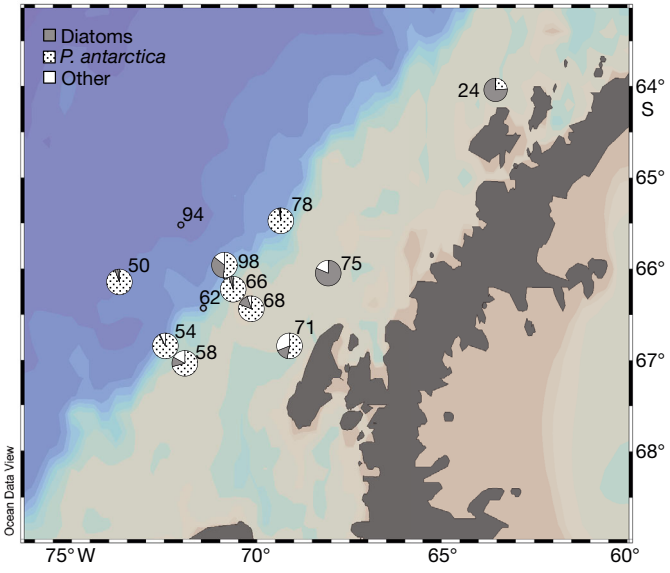

Fig. 1. Sea ice algal community composition in slush layers at ice stations in the western Antarctic Peninsula. Ice stations are noted by station numbers. Colors represent bathymetry, with the color contrast denoting the shelf break

Table 1. Geographic location and physical description of ice stations (see Fig. 1) sampled in the western Antarctic Peninsula; nd: no data. Freeboard: height of sea ice above sea level

Stn	Date (mo.d)	Lat (° S)	Long (° W)	Mean core depth (m, ± SD)	Mean snow depth (m, ± SD)	Ice temp (°C)	Mean salinity (± SD; non-slush layer)	Mean salinity (± SD; slush layer)	Freeboard (m)
24	11.3	64.027	63.584	0.45 ± 0.07	0.11 ± 0.02	nd	10 ± 1	15 ± 4	0.01
50	11.9	66.129	73.570	0.50 ± 0.14	0.06 ± 0.05	−1.30	5 ± 1	9 ± 1	0.03
54	11.10	66.798	72.240	0.69 ± 0.26	0.13 ± 0.04	nd	5 ± 1	11 ± 2	0.02
58	11.11	66.976	71.914	1.06 ± 0.10	0.08 ± 0.06	−1.00	5 ± 1	10 ± (nd)	0.08
62	11.12	66.429	71.438	0.60 ± 0.02	0.19 ± 0.07	−0.10	9 ± 3	14 ± 2	−0.01
66	11.13	66.086	70.831	0.88 ± 0.42	0.11 ± 0.05	−0.80	7 ± 2	12 ± 1	0.05
68	11.14	66.334	70.231	0.66 ± 0.01	0.13 ± 0.09	−2.70	10 ± 3	14 ± 1	0.02
71	11.15	66.838	69.088	1.18 ± 0.05	0.25 ± 0.13	−6.60	8 ± 2	13 ± 2	0.03
75	11.16	65.995	68.068	1.15 ± 0.57	0.35 ± 0.09	−1.80	9 ± 3	11 ± 6	−0.01
78	11.17	65.403	69.394	0.39 ± 0.01	0.09 ± 0.06	−1.10	7 ± 3	10 ± 0	0.01
94	11.20	65.517	72.049	0.42 ± 0.03	0.24 ± 0.06	−0.50	7 ± 2	nd	−0.05
98	11.21	66.051	70.899	0.80 ± 0.02	0.14 ± 0.04	−1.30	6 ± 2	10 ± (nd)	0.03

(Phantastic II) cruise (NBP14-09). Sea ice stations were established at or near main water column stations when the following were present: (1) sea ice and (2) suitable weather conditions. Sea ice and water column samples were collected between 3 and 21 November 2014.

On ice floes, snow thickness was measured using a meter stick at 15 randomly selected locations around the core site. Sea ice surface temperature was measured using a temperature probe at the snow–ice surface. Once ice cores were drilled, ice thickness was measured using a meter stick. Cores were cut into 0.1 m sections using a stainless steel ice saw, and the sections were placed in separate plastic containers to melt. Slush layers were sampled by scooping ice slush directly from the floe into plastic containers. All ice samples were stored in coolers until onboard processing for nutrients, biomass, and physiology. Immediately after returning to the ship, 0.2 µm filtered seawater (FSW) was added to ice samples (except ice cores analyzed for nutrients and salinity) to minimize osmotic shock to the ice algae during melt by maintaining salinity >28. Freeboard (f_b), the height of the sea ice above sea level, was calculated as $\rho_s h_s + \rho_i h_i = \rho_w (h_i - f_b)$ (Timco & Frederking 1996) using the density of seawater (ρ_w: 1029 kg m^{-3}), snow (ρ_s: 390 kg m^{-3}; Massom et al. 2001), and sea ice (ρ_i: 920 kg m^{-3}: Ackley et al. 2008) as well as the mean ice (h_i) and snow thicknesses (h_s) measured at ice stations.

Water column samples for growth and settling column experiments were collected from the CTD rosette at a depth of approximately 10 m at ice station locations. Both water column and ice samples underwent the same analyses: particulate organic carbon (POC), particulate organic nitrogen (PON), chl *a* and other algal pigments, taxonomic composition (using CHEMTAX-HPLC and FlowCam), photophysiological parameters (quantified using photosynthesis vs. irradiance curves (PvE) and fast rate repetition fluorometry (FRRF)), and salinity and nutrients (silicate ($Si(OH)_4$), nitrate (NO_3^-), and phosphate (PO_4^{3-})).

Growth experiments (shipboard incubations)

To determine the viability of ice algae that melted out of the slush layer relative to water column phytoplankton under sustained high and low light levels, we conducted 6 d shipboard incubation experiments in a temperature- (0°C) and light-controlled incubator. Experiments were conducted on 3, 10, and 17 November 2014 using ice algae (from the slush layer) and seawater (from 10 to 20 m) collected at Stations (Stns) 24, 54, and 78 (Fig. 1). Slush samples collected at ice stations for experiments were melted in 4 l of FSW to maintain salinities >32. Samples from the ice and water column were incubated in 4 l Whirl-Pak bags (Nasco). Because of the large biomass concentration differences between ice and seawater, we further diluted slush ice samples with ~3.7 l of 0.2 µm FSW (~34 salinity) collected near ice stations to match biomass concentrations in seawater samples. Dilutions were calculated from *in vivo* fluorescence of ice and seawater to achieve the same biomass concentrations in ice and seawater samples. Triplicate samples (mean ± SD) were incubated under either high (200 ± 31 µmol photon m^{-2} s^{-1}) or low (91 ± 25 µmol photon m^{-2} s^{-1}) light. The high light level was similar to the mean light in a shallow mixed layer (ML) (250 µmol photon m^{-2} s^{-1}, Mills et al. 2010) and summer MLs in the Ross Sea (180 ± 110 µmol photon m^{-2} s^{-1}, Smith & van Hilst 2003). The low light level was similar to the mean light in a deep ML (65 µmol photon m^{-2} s^{-1}, Mills et al. 2010) and mid to late spring MLs in the Ross Sea (96 ± 58 µmol photon m^{-2} s^{-1}). Experiment 1 (Expt 1) was conducted under a 12 h light:12 h dark cycle. Maintaining a 12:12 h light cycle was not possible after Expt 1. Expts 2 and 3 were conducted under 24 h light. Treatments were subsampled on Days 0 (T0), 4 (T4), and 6 (T6) for $Si(OH)_4$, NO_3^-, PO_4^{3-}, POC, PON, chl *a*, other algal pigments, taxonomic composition, and photophysiological parameters. To ensure that treatments remained in nutrient-replete conditions over the 6 d experiment, we replaced the water removed for sampling at T4 with 2 l of FSW. Growth rates (r) were calculated, assuming exponential growth ($B_F = B_0 \times e^{(rt)}$) over 2 d ($t$), where B_0 and B_F are the initial and final biomass, respectively

Statistical differences among treatments in the growth experiment were analyzed using a 2-way analysis of variance (ANOVA; R). Main effects included light level (high versus low) and community type (ice algae versus phytoplankton). When the 2-way ANOVA interaction term (light × community type) was significant ($p < 0.05$), differences among treatments were analyzed using the Tukey honestly significant difference (HSD) test. Statistical differences between T0 and T6 measurements were analyzed using a paired *t*-test.

Settling column experiments

To determine the export potential of ice algae and phytoplankton, we conducted settling column exper-

iments in duplicate or triplicate (n = 2, 3) using samples collected from the sea ice slush layer (Stns 50, 58, 62, 66, 68, 71, 78) and near surface waters (Stns 2, 15, 38, 40, 44, 48). Conducting simultaneous ice algal and phytoplankton settling experiments was not possible due to the limited number of settling columns. Settling columns were constructed out of capped polycarbonate tubes (diameter = 0.07 m, length = 0.46 m) with 3 sampling ports positioned to collect buoyant, neutral, and settled particles, following Johnson & Smith (1986) and Bienfang (1981). Experiments were conducted in a temperature (0°C) and light (~60 µmol photon m^{-2} s^{-1}) controlled incubator. Samples from the water column and sea ice were added to the settling columns in duplicate or triplicate and then sampled for chl *a* at each port after ~24 h. For a limited number of stations, settling column experiments were sampled after 2 h (Stns 2 and 40), 4 h (Stns 15, 38, 40, and 58), 8 h (Stn 15), and 15 h (Stns 44 and 50) to assess how well sinking rates were estimated after 24 h. A subset of samples was also analyzed for taxonomic composition. Sinking rate (ψ, m d^{-1}) was calculated from the equation of Bienfang (1981), modified by Johnson & Smith (1986):

$$\psi = f_s \times l/t \quad (1)$$

where f_s is the fraction of chl *a* that sank over the length of the column (l, m) during the settling period (t, d).

Sample analyses

Nutrients

Inorganic nutrient samples were filtered with a 0.2 µm syringe filter and stored at −20°C (NO_3, PO_4^{3-}) or 4°C ($Si(OH)_4$) for later analysis upon return. NO_3^- and $Si(OH)_4$ concentrations were analyzed at the Royal Netherlands Institute for Sea Research (NIOZ) on a WestCo SmartChem 200 discrete autoanalyzer.

Pigments, POC, and PON

Samples were collected by filtering seawater or melted sea ice through 25 mm Whatman glass-fiber filters (GF/F, nominal pore size 0.7 µm). Chl *a* was measured in triplicate using a Turner 10-AU fluorometer (Turner Designs) after extraction in 5 ml of 90% acetone in the dark at 3°C for 24 h (Holm-Hansen et al. 1965). The fluorometer was calibrated using a pure chl *a* standard (Sigma).

Samples were analyzed for phytoplankton pigments by HPLC, as described below. Filters were freeze-dried for 48 h and pigments were extracted using 90% acetone (v/v) for 48 h (4°C, in the dark). Pigments were separated by HPLC (Waters 2695) with a Zorbax Eclipse XDB-C8 column (3.5 µm particle size), using the method of Van Heukelem & Thomas (2001). Detection was based on retention time and diode array spectroscopy (Waters 996) at 436 nm. Pigments were manually quantified using standards (DHI lab products). Analyzed pigments include chlorophylls: *a*, *b*, c_2, c_3, photoprotective index pigments (PPC: diadinoxanthin [DD], diatoxanthin [DT], violaxanthin [Viola], zeaxanthin [Zea], lutein, and beta-carotene), and taxonomic marker pigments (peridinin [Per], 19-butanoyloxyfucoxanthin [19-But], 19-hexanoyloxyfucoxanthin [19-Hex], fucoxanthin [Fuco], and alloxanthin [Allo]). Community composition was estimated from pigments (HPLC) using the CHEMTAX analysis package (version 1.95) (Mackey et al. 1996) (Table A1 in the Appendix). Taxonomic composition of CHEMTAX-HPLC is compared to the FlowCam analyses in the 'Results' and is presented in the 'Results' and 'Discussion' from the FlowCam analyses.

POC and PON samples were filtered onto pre-combusted (450°C for 4 h) GF/Fs. Filters were dried at 60°C for approximately 24 h and then stored for later elemental analysis on a Elementar Vario El Cube or Micro Cube elemental analyzer (Elementar Analysensysteme) interfaced to a PDZ Europa 20-20 isotope ratio mass spectrometer (Sercon). The concentration of POC and PON in the sea ice was then calculated from the known volumes of melted sea ice and the FSW diluent water additions.

Photosynthesis versus irradiance curves

PvE measurements were made using a short-term (2 h) ^{14}C-bicarbonate uptake technique (following Lewis & Smith 1983, modified by Arrigo et al. 2010) on samples collected from the sea ice and the water column. PvE measurements were made (n = 1; 1 measurement per sample due to time constraints and space limitations) on high biomass layers of the sea ice and growth experiment treatments.

Samples spiked with ^{14}C-bicarbonate were incubated under 14 light intensities ranging from 0 to 700 µmol photon m^{-2} s^{-1}. Carbon uptake rates were calculated using a nonlinear least-squares regression fit to the relationship of Platt et al. (1980), as modified by Arrigo et al. (2010):

$$P^{\star} = P_s^{\star}\left(1 - e^{\frac{-\alpha^{\star}E}{P_s^{\star}}}\right)e^{\frac{-\beta^{\star}E}{P_s^{\star}}} - P_0^{\star} \quad (2)$$

where $P^{\star}$ is the chl *a*-specific (as denoted by *) photosynthetic rate (mg C mg^{-1} chl *a* h^{-1}) at a given irradiance E (µmol photon m^{-2} s^{-1}), $P_s^{\star}$ is the light saturated photosynthetic rate (mg C mg^{-1} chl *a* h^{-1}) in the absence of photoinhibition, $\alpha^{\star}$ is the initial slope of the PvE curve (mg C mg^{-1} chl *a* h^{-1} (µmol photon m^{-2} s^{-1})$^{-1}$), $P_0^{\star}$ is the rate of dissolved inorganic carbon uptake in the dark, and $\beta^{\star}$ is the photoinhibition term at high light (mg C mg^{-1} chl *a* h^{-1} (µmol photon m^{-2} s^{-1})$^{-1}$). The maximum photosynthetic rate in the absence of photoinhibition ($P_m^{\star}$) was then calculated from:

$$P_m^{\star} = P_s^{\star}\left(\frac{\alpha^{\star}}{\alpha^{\star}+\beta^{\star}}\right)\left(\frac{\beta^{\star}}{\alpha^{\star}+\beta^{\star}}\right)^{\frac{\beta^{\star}}{\alpha^{\star}}} \quad (3)$$

PvE parameters were only used when fits were significant ($r^2 > 0.7$ and $p < 0.05$). The photoacclimation parameter (E_k; µmol photon m^{-2} s^{-1}), was calculated as $P_m^{\star}/\alpha^{\star}$.

FRRF measurements

Melted and diluted ice samples (as described above) from 0.1 m core sections, water column samples, and growth experiment treatment samples were dark acclimated for 30 min at 0°C before measuring fluorescence. Blanks were prepared by filtering the sample through a 0.2 µm polycarbonate syringe filter. Variable fluorescence parameters of blanks and samples were measured using a bench top fast repetition rate fluorometer (LIFT-FRR, Soliense; Kolber et al. 1998) at an excitation wavelength of 470 nm. Blank-corrected values (Cullen & Davis 2003) for initial fluorescence (F_o), maximum fluorescence (F_m), and the effective absorption cross section (σ, Å^2 quanta^{-1}) give information on the photophysiology of Photosystem II (PSII). Fluorescence measurements were used to calculate the maximum quantum efficiency of PSII (F_v/F_m; Maxwell & Johnson 2000).

FlowCam analyses

Samples were collected and analyzed from slush and non-slush ice core sections, settling column experiments, and growth experiment treatments (T0 and T6). Nano- and micro-size phytoplankton and ice algae were imaged with a FlowCam (VS IVc, Fluid Imaging Technologies) under 40× magnification. To prevent large cells from clogging the flow cell chamber, samples were pre-filtered with 300 µm Nitex mesh. Particles in seawater or melted ice core (1 to 5 ml sample) flowed through a flow cell, and each fluorescent chain, colony, or cell triggered the digital camera. The combination of the size of the Nitex mesh, the size of the flow cell chamber, and the fluorescence trigger sensitivity limited the FlowCam detection range to particle sizes of 5 to 300 µm. Digital images were classified manually into pennate and centric diatom taxa, *P. antarctica,* dinoflagellates, ciliates, small unidentified cells, and other.

Biovolume calculations are prone to error, as 2-dimensional images are used to estimate the volume of a 3-dimensional shape (Álvarez et al. 2012), and plankton cells captured by the camera can be singular or part of a chain or colony and in a variety of orientations (Jakobsen & Carstensen 2011). For all taxonomic categories other than *P. antarctica*, biovolume calculations were made using geometric shape equations following Menden-Deuer & Lessard (2000) and Jakobsen & Carstensen (2011). *P. antarctica* cells per image within a *P. antarctica* colony were estimated using a multiple linear regression model ($R^2 = 0.95$, $p < 0.001$, parameter coefficients specified below) based on the following FlowCam image parameters: area-based diameter ($\beta = 8.402 \times 10^{-3}$, $p < 0.001$) and convex perimeter ($\beta = 8.235 \times 10^{-2}$, $p < 0.001$), which were selected using results from a best subsets model analysis (Bayesian Information Criteria) of 1000 images. To evaluate model skill, a separate set of images (1000) was tested against the predicted values (Fig. A1 in the Appendix). Colony volume calculations were made from cell number estimations following Mathot et al. (2000). We did not assess single-celled *P. antarctica* because we could not distinguish small *P. antarctica* cells and other unidentifiable small cells. Taxonomic composition is presented in the results and discussion from FlowCam analysis as relative abundance, estimated from biovolume.

RESULTS

Physical and chemical ice environment

The ice stations were characterized by many small pancake ice floes (diameter ≈ 3–6 m) ranging in thickness from 0.42 to 1.18 m (mean 0.73 ± 0.28 m) that were sometimes rafted and covered by thick snow (Table 1). Freeboard, the height of the ice floe above sea level, ranged from –0.05 to 0.08 m, sug-

gesting that 95% or greater of the ice floe was submerged at all ice stations (Table 1). Mean snow depth at each station ranged from 0.06 to 0.35 m, with 75% of stations exceeding 0.10 m of snow cover. Ice floe surfaces consisted of snow, slush, and/or ice, with surface temperatures ranging from −6°C to the melting point. Mean bulk salinities ranged from 5 to 10 in non-slush layers and from 9 to 15 in slush layers within ice cores (Table 1).

The vertical distributions of bulk nutrient concentrations were highly variable throughout the sea ice across the WAP, ranging from 0.09 to 13.42 µM NO_3^-, 0.17 to 3.14 µM PO_4^{3-}, and 0 to 28.28 uM $Si(OH)_4$ (Fig. 2A–C). The ratios of observed nutrient concentrations to those expected by conservative mixing with seawater show where nutrients may be biologically elevated or depleted throughout the core profile (Fig. 2D–F). Conservative mixing ratios for bulk NO_3^- and $Si(OH)_4$ were often <1, indicating net drawdown (Fig. 2D,F), while PO_4^{3-} ratios were often >1, indicating enhanced remineralization or the presence of large algal intracellular phosphate pools within the sea ice (Fig. 2E).

Ice algal bloom

Biomass

Depth-integrated chl *a* for all sea ice stations ranged from 5 to 120 mg m^{-2}, averaging 38 ± 34 mg m^{-2} (Table 2). Depth-integrated POC and PON ranged from 2.8 to 15.6 g C m^{-2} and 0.3 to 1.9 g C m^{-2}, respectively (Table 2). POC and PON were positively correlated ($y = 6.87x + 1182$, $R^2 = 0.90$, $p < 0.05$; Fig. A2 in the Appendix) with an average POC:PON ratio of 9.1 ± 1.8 (Table 2). In contrast, POC and chl *a* were not correlated, with POC:chl *a* ratios ranging from 59.0 to 843.3, with a median of 168.4 (Table 2). Depth-integrated biomass proxies (chl *a*, POC, PON) were not significantly correlated with snow depth, ice thickness, or ice temperature.

Biomass was vertically divided into surface (top 0.1 m at ice–snow interface), interior (non-slush layers between the surface and bottom of the ice core), bottom (0.1 m at ice–ocean interface) or slush layers (identified from visual inspection). Often biomass was concentrated in thick slush layers (>0.1 m) that

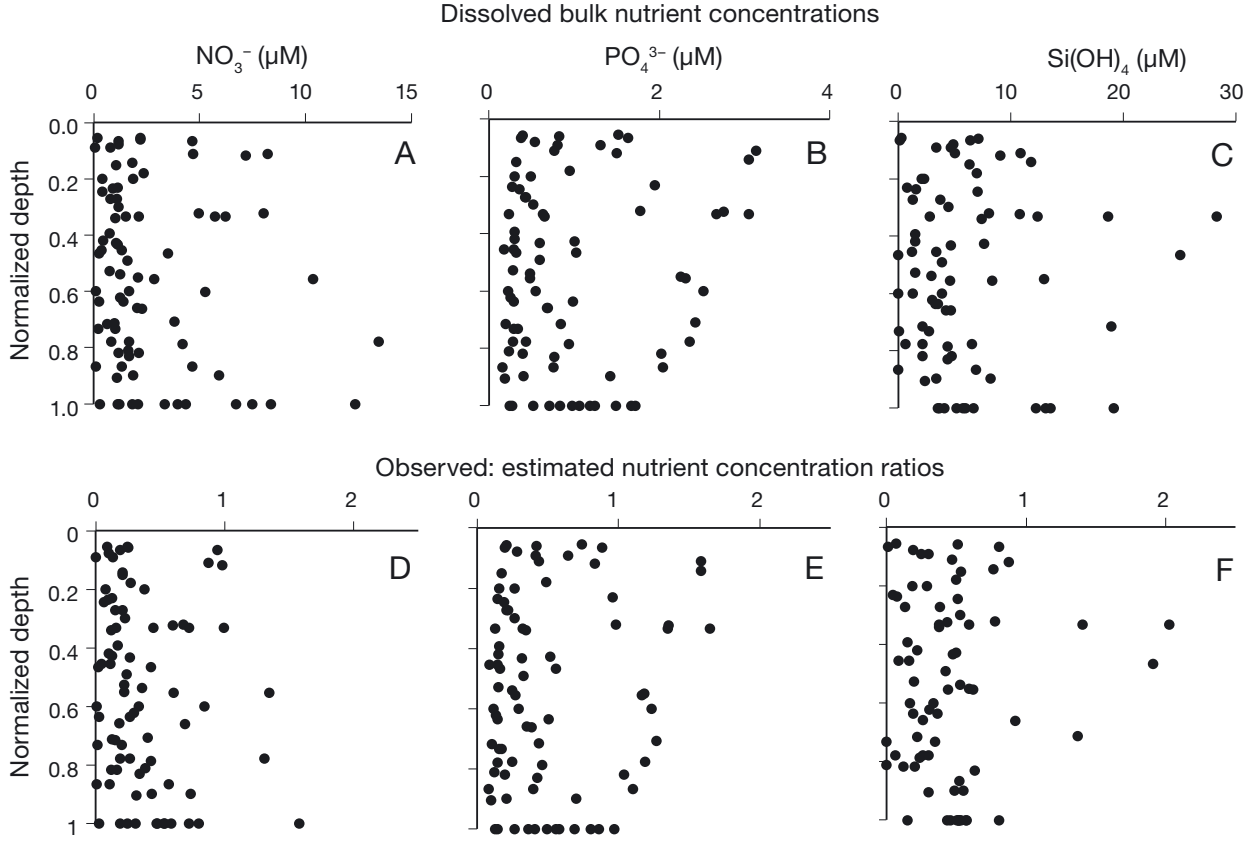

Fig. 2. (A–C) Ice core bulk nutrient profiles distributed through the normalized ice core depth (1.0 is the ice–ocean interface). (D–F) Profiles of observed to estimated (assuming conservative mixing with seawater) nutrient concentration ratios distributed through the normalized ice core depth

Table 2. Depth-integrated biomass of ice algae (mg m^{-2}) and photosynthesis-irradiance parameters (PvE) of a single high biomass layer in the ice core (slush or non slush) at each ice station. POC (PON): particulate organic carbon (nitrogen); P_m^* (mg C mg^{-1} chl *a* h^{-1}): maximum photosynthetic rate; α^* (mg C mg^{-1} chl a h^{-1} (µmol photon m^2 $s^{-1})^{-1}$): initial slope of the PvE curve; E_k (µmol photon m^2 s^{-1}): photoacclimation parameter; nd: no data

Station	Biomass			PvE parameters		
	Chl *a*	POC	PON	P_m^*	α^*	E_k
24	18	nd	nd	nd	nd	nd
50	20	6898	665	0.60	0.006	95
54	5	2850	260	0.21	0.005	45
58	27	4467	446	0.05	0.001	36
62	14	3433	279	nd	nd	nd
66	120	15561	1726	2.90	0.043	68
68	67	6102	600	1.51	0.020	74
71	23	2791	331	1.18	0.034	34
75	87	5121	692	0.16	0.009	16
78	36	3117	433	3.14	0.033	95
94	14	12019	1920	0.28	0.001	274
98	26	4820	538	0.78	0.026	30

were brown in color and sometimes divided into multiple slush layers within an ice core (Fig. 3). Our biomass measurements of the slush layer are conservative because sample collection resulted in some unquantified dilution with ambient seawater. Here, we present the volumetric concentration of biomass (mg m^{-3}) and the biomass concentration over the vertical extent of the slush layer (mg m^{-2}). Mean slush layer chl *a* (8.8 ± 1.9 mg m^{-2} [72 ± 11 mg m^{-3}]) and PON (136 ± 75 mg m^{-2} [1368 ± 641 mg m^{-3}]) concentrations were 2 to 3 times higher than those in the nonslush layers of the core, which included the mean of surface, interior, and bottom communities (3.2 ± 0.9 mg chl *a* m^{-2} [34 ± 7 mg m^{-3}] and 56 ± 3 mg PON m^{-2} [651 ± 63 mg m^{-3}]; Fig. 3). In contrast, differences between slush and non-slush mean POC were small. Slush layers were characterized by lower POC:chl *a* ratios (136 ± 45) and POC:PON (7 ± 0.5) ratios relative to the rest of the core (300 ± 24 POC:chl *a*, 10 ± 0.4 POC:PON; Table 3).

Photophysiological state

Algae living within slush communities exhibited different photophysiological parameters than those in non-slush layers (surface, interior, and bottom) of the core (Table 3). The P_m^* of ice algal communities ranged from 0.03 (interior layer, data not shown) to 3.14 mg C mg^{-1} chl *a* h^{-1} (high biomass slush layer, Table 2). Within that range, mean P_m^* of slush communities (1.19 ± 0.34 mg C mg^{-1} chl *a* h^{-1}) was 8 times greater than the rest of the core (0.15 ± 0.04 mg C mg^{-1} chl *a* h^{-1}; Table 3). The photosynthetic efficiency (α^*) of ice algal communities ranged from <0.001 (interior layer, data not shown) to 0.043 mg C mg^{-1} chl *a* (µmol photon m^{-2} $s^{-1})^{-1}$ (slush layer, Table 2). The slush community mean α^* (0.021 ± 0.004 mg C mg^{-1} chl *a* (µmol photon m^{-2} $s^{-1})^{-1}$) was an order of magnitude greater than that of the rest of the core (0.002 ± 0.001 mg C mg^{-1} chl *a* (µmol photon m^{-2} $s^{-1})^{-1}$) (Table 3). Despite the differences in P_m^* and α^* between the slush and non-slush communities, the mean photoacclimation levels (E_k) for the non-slush (89 ± 24 µmol photon m^{-2} s^{-1}) and slush (55 ± 9 µmol photon m^{-2} s^{-1}) communities were not significantly different (Table 3). Overall, E_k ranged from 16 to 274 µmol photon m^{-2} s^{-1} between the ice communities.

There were no significant differences between slush and non-slush layer PSII parameters. Overall, F_v/F_m was low for slush layers and non-slush layers (0.344 ± 0.027 and 0.306 ± 0.013, respectively) and the mean absorption cross-sections (σ_{PSII}) were similar (830 ± 37 and 897 ± 18 $Å^2$ $quanta^{-1}$, respectively;

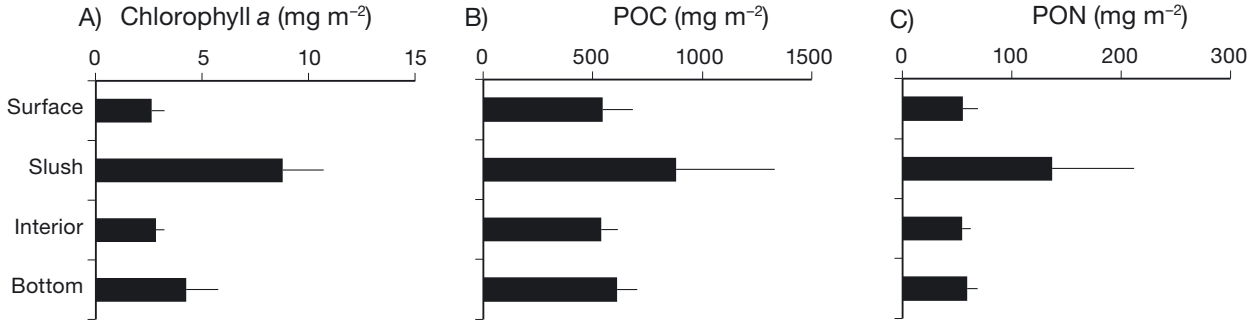

Fig. 3. Mean ± SE depth profiles of biomass (mg m^{-2}) for the surface, slush, interior, and bottom layers of the sea ice: (A) chlorophyll *a* (chl *a*), (B) particulate organic carbon (POC), and (C) particulate organic nitrogen (PON). Ice core profiles are divided into: surface (0.1 m; ice–snow interface), slush (visually identified), interior (layers between the top and bottom), and bottom (0.1 m; ice–ocean interface)

Table 3. Mean (± SE) ice algal community parameters for non-slush (n = 9) and slush layers (n = 11). Non-slush layers include those sampled from bottom, interior, and surface communities. POC (PON): particulate organic carbon (nitrogen); $P_m^{\star}$: maximum photosynthetic rate; $\alpha^{\star}$: initial slope of the photosynthesis-irradiance parameter (PvE) curve; E_k: photoacclimation parameter; F_v/F_m: Photosystem II efficiency; σ: functional absorption cross-section; PPC: photoprotective index pigments

Parameter	Unit	Slush	Non-slush
Biomass and physiology			
POC:chl *a*[a]	g:g	136 ± 45	300 ± 24
POC:PON[a]	g:g	7 ± 0.5	10 ± 0.4
$P_m^{\star}$[a]	mg C mg^{-1} chl *a* h^{-1}	1.19 ± 0.34	0.15 ± 0.04
$\alpha^{\star}$[a]	mg C mg^{-1} chl *a* h^{-1} (µmol photon m^2 s^{-1})$^{-1}$	0.021± 0.004	0.002 ± 0.001
E_k	µmol photon m^2 s^{-1}	55 ± 9	89 ± 24
F_v/F_m		0.344 ± 0.027	0.306 ± 0.013
σ	Å^2 quanta^{-1}	830 ± 37	897 ± 18
PPC:chl *a*	g:g	0.18 ± 0.02	0.20 ± 0.01
Taxonomic composition (relative abundance)			
Colonial *Phaeocystis antarctica*		0.69 ± 0.10	0.60 ± 0.11
Diatoms		0.22 ± 0.09	0.15 ± 0.06
Other		0.09 ± 0.03	0.25 ± 0.11

[a]*t*-test, $p < 0.05$

Table 3). Photoprotective carotenoid pigment (PPC) to chl *a* ratios were also similar (Table 3). Diadinoxanthin + diatoxanthin comprised 95% of the PPC pigments in both slush and non-slush ice algal communities.

Ice algal community composition

Estimates of the relative proportions of dominant taxa (>50%) from FlowCam and CHEMTAX-HPLC analyses were in general agreement (Fig. A1). Overall, CHEMTAX-HPLC analysis estimated lower relative abundance of *Phaeocystis antarctica* than FlowCam analysis. FlowCam imaging indicated that *P. antarctica* populations were largely colonial, rather than single-celled, and comparison of the 2 methods suggests that *P. antarctica* was adequately counted. Both methods showed that diatoms and haptophytes (*P. antarctica*) dominated all samples, and CHEMTAX HPLC showed that prasinophytes, dinoflagellates, and cryptophytes comprised <1% of the algal community.

The community composition of high-biomass layers in the slush and non-slush layers (bottom, interior, or surface) of the sea ice was consistently dominated by *P. antarctica* (estimated by biovolume, µm^3; Fig. 1, Table 3). Mean relative abundances of *P. antarctica* and diatoms in slush and non-slush layers were not significantly different (Table 3). In contrast to the majority of stations, ice algal communities at Stns 24 and 75 were dominated by diatoms rather than *P. antarctica* (Fig. 1). Diatoms were primarily centrics (*Thalassiosira*), followed by large pennate diatoms (*Fragilariopsis*) and small unidentified pennate diatoms. Other diatoms, including *Chaetoceros, Nitzschia, Pseudo-nitzschia, Proboscia, Rhizosolenia,* and *Skeletonema,* composed a minor fraction of the total biovolume.

Growth experiments

To understand how ice algae (post-ice melt) and phytoplankton respond to changes in their light environment, we exposed both communities to high and low light levels over 6 d incubations (Expts 1–3). Expt 1 differed in initial community composition (mixed diatom–*P. antarctica*) and light condition (12:12 h) from Expts 2 and 3 (*P. antarctica* dominant, 24 h continuous light) and is treated separately.

Community composition

12:12 h light cycle (*Expt 1*). Initial (T0) communities were mostly composed of centric diatoms. *P. antarctica* was also present and made up a higher percentage of the ice algal community than the phytoplankton community (Fig. 4A). Ice and phytoplankton centric diatom communities were predominantly made up of *Thalassiosira* (>75%). *Corethron* also contributed 20% to the centric phytoplankton biomass. At T6, relative abundance (estimated by biovolume) of *P. antarctica* had increased and diatoms decreased in all treatments (Fig. 4A).

24 h light cycle (*Expts 2 and 3*). While diatoms dominated the T0 communities of Expt 1, the T0 communities of Expt 2 (24 h light conditions) consisted of a mix of diatoms and *P. antarctica* (Fig. 4B). Similar to Expt 1, *P. antarctica* made up a larger percentage of the ice algae (67%) than the phytoplankton community (40%) in Expt 2. There were greater differences between the diatom communities of the ice algae and phytoplankton in Expt 2 than in Expt 1. Ice algae diatoms were composed of *Fragilariopsis* (12%) and *Thalassiosira* (17%), while phytoplankton diatoms were predominantly made up of *Thalassiosira* (45%), *Chaetoceros* (9%), and *Corethron* (19%). In contrast to Expts 1 and 2, in Expt 3 *P. antarctica* dominated the initial ice algae (94%) and phytoplankton (92%) communities. Within both communities, *Thalassio-*

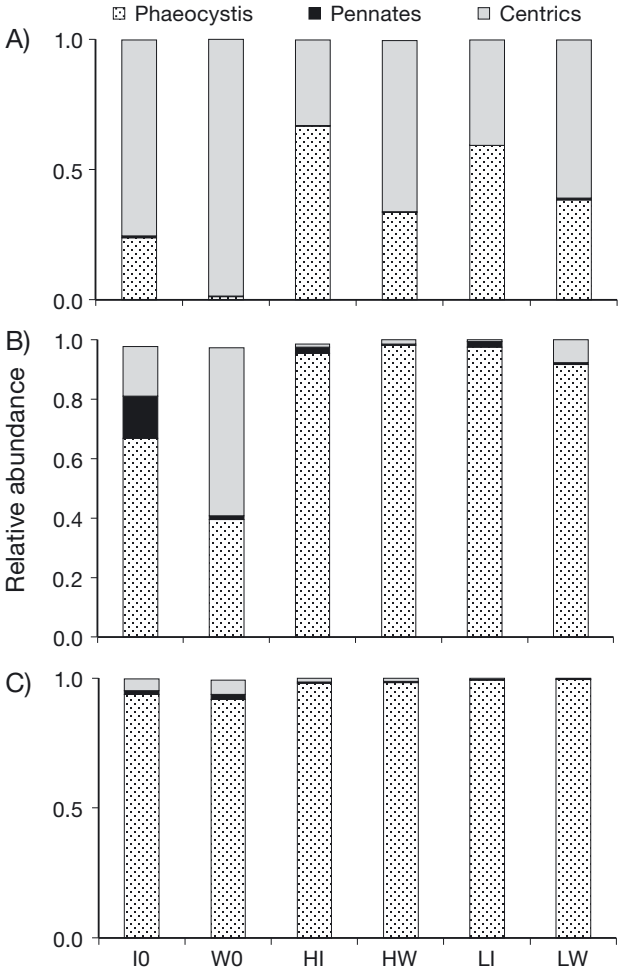

Fig. 4. Taxonomic composition of ice algal (I) and phytoplankton (W) communities incubated in high (H) and low (L) light on Day 6 of growth experiments (0 indicates Day 0). Relative abundance of *Phaeocystis antarctica* and diatoms (pennates and centrics) is estimated from biovolume measurements from FlowCam for growth experiments: (A) Expt 1, (B) Expt 2, and (C) Expt 3

sira represented the majority of diatoms in Expt 3 (Fig. 4C). At T6, in both Expts 2 and 3, relative abundance of *P. antarctica* had increased and diatoms decreased in all treatments (Fig. 4B,C)

Growth and physiology parameters

12:12 h light cycle (*Expt 1*). Phytoplankton tended to grow faster than ice algae under 12:12 h light, indicated by chl *a*-based (2-way ANOVA, $p < 0.001$) and POC-based growth estimates (Table 4). Furthermore, phytoplankton were more sensitive to light treatments than ice algae, growing faster in high light (1.18 d^{-1}) than in all other treatments (Tukey HSD, $p < 0.05$). At T0, ice algae were acclimated to higher light levels (E_k: 84 µmol photon m^{-2} s^{-1}) than phytoplankton (E_k: 47 µmol photon m^{-2} s^{-1}). At T6, E_k in these communities was similar, within 10 µmol photon m^{-2} s^{-1} for both light treatments (Fig. 5A). Despite similarities in E_k, ice algae and phytoplankton exhibited differences in $\alpha^\star$ and $P_m^\star$, depending on light level (Fig. 5B,C). At T6 in high light, ice algae had higher $\alpha^\star$ (0.03 mg C mg^{-1} chl *a* h^{-1} (µmol photon m^{-2} $s^{-1})^{-1}$) and $P_m^\star$ (1.95 mg C mg^{-1} chl *a* h^{-1}) than phytoplankton (0.016 mg C mg^{-1} chl *a* h^{-1}(mol photon m^{-2} $s^{-1})^{-1}$, 1.03 mg C mg^{-1} chl *a* h^{-1}). In low light at T6, trends were opposite those of high light conditions: ice algae had lower $\alpha^\star$ (0.04 mg C mg^{-1} chl *a* h^{-1} (µmol photon m^{-2} $s^{-1})^{-1}$) and $P_m^\star$ (1.92 mg C mg^{-1} chl *a* h^{-1}) than phytoplankton (0.05 mg C mg^{-1} chl *a* h^{-1} (µmol photon m^{-2} $s^{-1})^{-1}$ and 2.33 mg C mg^{-1} chl *a* h^{-1}, respectively).

Initially, ice algae had lower F_v/F_m and σ_{PSII} than phytoplankton (Fig. 5D,E). From T0 to T6, phytoplankton maintained higher F_v/F_m than ice algae, but under both light levels, F_v/F_m of ice algae increased (2-way ANOVA, $p < 0.001$; *t*-test, $p < 0.05$). Both communities decreased σ_{PSII} (*t*-test, $p < 0.05$) to similar values at T6. Ice algae and phytoplankton also had similar PPC:chl *a* ratios at T6 (Fig. 5F). T0 compar-

Table 4. 2-way ANOVA on the influence of 2 independent variables (light level and community type) on community growth rates calculated from changes in chl *a* and POC assuming exponential growth, as defined in 'Materials and methods' (mean ± SD) for water column phytoplankton (W) and sea ice algae (I) communities. Significant main effects are marked with ⋆ (for Type). When the interaction term (Light × Type) was significant, a Tukey HSD was performed on all combinations. Differences from the Tukey HSD are represented by superscripts A, B, and C; nd: no data; POC: particulate organic carbon

Experiment	Light level	Type	Chl *a* (d^{-1})	POC (d^{-1})
Expt 1 (12:12 h)	High	W	1.18 ± 0.08^A	0.62 ± 0.10
		I	0.47 ± 0.01^B	0.53 ± 0.06
	Low	W	0.80 ± 0.06^C	0.74 ± 0.07
		I	0.46 ± 0.11^B	nd
Expt 2 (24 h)	High	W	0.62 ± 0.03	0.75 ± 0.01
		I	0.76 ± 0.09	0.88 ± 0.06
	Low	W	0.73 ± 0.20	0.61 ± 0.10
		I	0.81 ± 0.09	0.89 ± 0.18
Expt 3 (24 h)	High	W	$0.54 \pm 0.03^\star$	0.64 ± 0.07
		I	$1.26 \pm 0.50^\star$	0.89 ± 0.03
	Low	W	$0.63 \pm 0.07^\star$	0.76 ± 0.14
		I	$0.94 \pm 0.09^\star$	1.14 ± 0.25

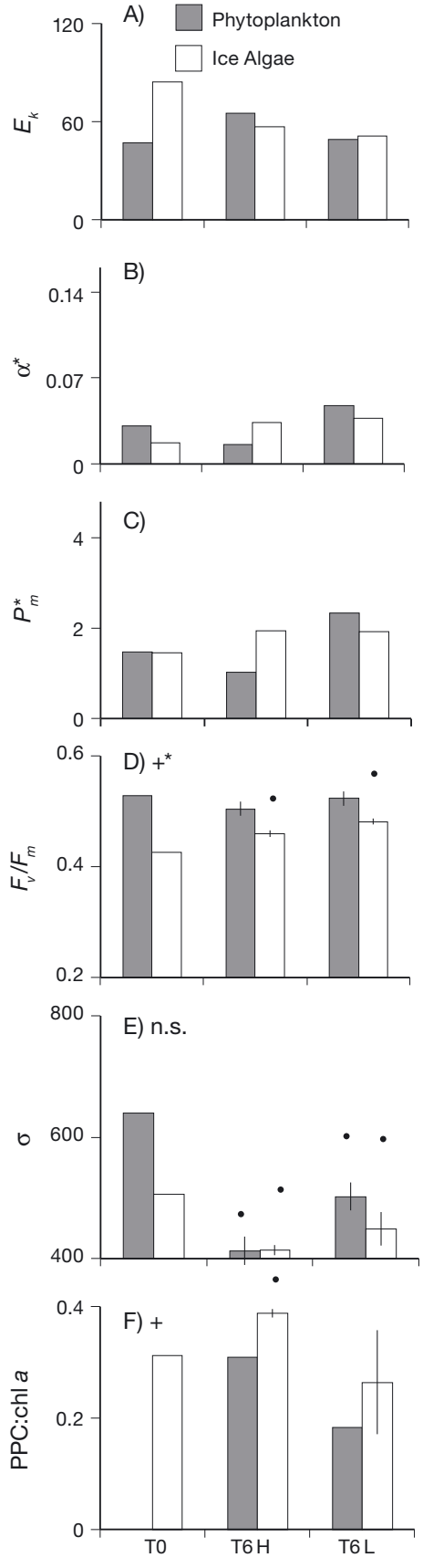

isons of photoprotective pigment to chl *a* (PPC:chl *a*) ratios were not available.

24 h light cycle (*Expts 2 and 3*). Ice algal communities grown under 24 h continuous light tended to have higher chl *a*-based (Expt 3: 2-way ANOVA, $p < 0.05$) and POC-based growth rates than phytoplankton (Table 4). At T0, ice algae exhibited higher E_k (Expt 2: 90 µmol photon m^{-2} s^{-1}) than phytoplankton (27 and 17 µmol photon m^{-2} s^{-1} for Expts 2 and 3, respectively; Fig. 6A,B). At T6, ice algae maintained a higher E_k than phytoplankton in both the high and low light treatments. Initially, ice algae α^* (Expt 2: 0.02 mg C mg^{-1} chl *a* h^{-1} (µmol photon m^{-2} $s^{-1})^{-1})$ was lower than that of phytoplankton (Expt 2: 0.13 mg C mg^{-1} chl *a* h^{-1} (µmol photon m^{-2} $s^{-1})^{-1}$; Fig. 6C). At T6, ice algae and phytoplankton α^* were similar (Fig. 6C,D). Initial P^*_m tended to be lower for ice algae (Expt 2: 2.11 mg C mg^{-1} chl *a* h^{-1}) than for phytoplankton (3.65 and 2.79 mg C mg^{-1} chl *a* h^{-1} for Expts 2 and 3, respectively; Fig. 6E,F). At T6, ice algae had higher P^*_m than phytoplankton in all light treatments (Expts 2 and 3).

Initially, for Expts 2 and 3, respectively, ice algae tended to have lower F_v/F_m (0.410 and 0.358) and σ_{PSII} (507 and 661 $Å^2$ $quanta^{-1}$) and higher PPC:chl *a* ratios (0.25 and 0.26) than phytoplankton (F_v/F_m: 0.480 and 0.471; σ_{PSII}: 717 and 617 $Å^2$ $quanta^{-1}$; PPC:chl *a* ratios: 0.08 and 0.10) (Fig. 6G–L). By T6, ice algae and phytoplankton had similar F_v/F_m and σ_{PSII}. While ice algae and phytoplankton PSII parameters were similar, ice algae PPC:chl *a* ratios were significantly lower than those of phytoplankton (2-way ANOVA, $p < 0.001$, $p < 0.001$ for Expts 2 and 3, respectively).

Settling column experiments

We also explored the role differential sinking may have on the contribution of ice algae to phytoplankton

Fig. 5. Photophysiology parameters (mean, with ± SD shown in D–F T6) of ice algae and phytoplankton for Expt 1 (12:12 h) on Day 0 (T0) and Day 6 (T6) incubated under high (H) and low (L) light levels: (A) photoacclimation parameter (E_k, µmol photon m^2 s^{-1}), (B) photosynthetic efficiency (α^*, mg C mg^{-1} chl *a* h^{-1} (µmol photon m^2 $s^{-1})^{-1}$), (C) maximum photosynthetic rate (P^*_m, mg C mg^{-1} chl *a* h^{-1}), (D) Photosystem II efficiency (F_v/F_m), (E) functional absorption cross-section (σ_{PSII}, $Å^2$ $quanta^{-1}$), and (F) photoprotective pigment (PPC):chl *a* ratios. A 2-way ANOVA was conducted on the influence of 2 independent variables (light level and community type, where significant results are marked with + or *, respectively) on F_v/F_m, σ, and pigment ratios. A paired *t*-test ($p < 0.05$) was used to assess the change between T0 and T6, and black dots above the treatments (H or L) represent a significant change from T0

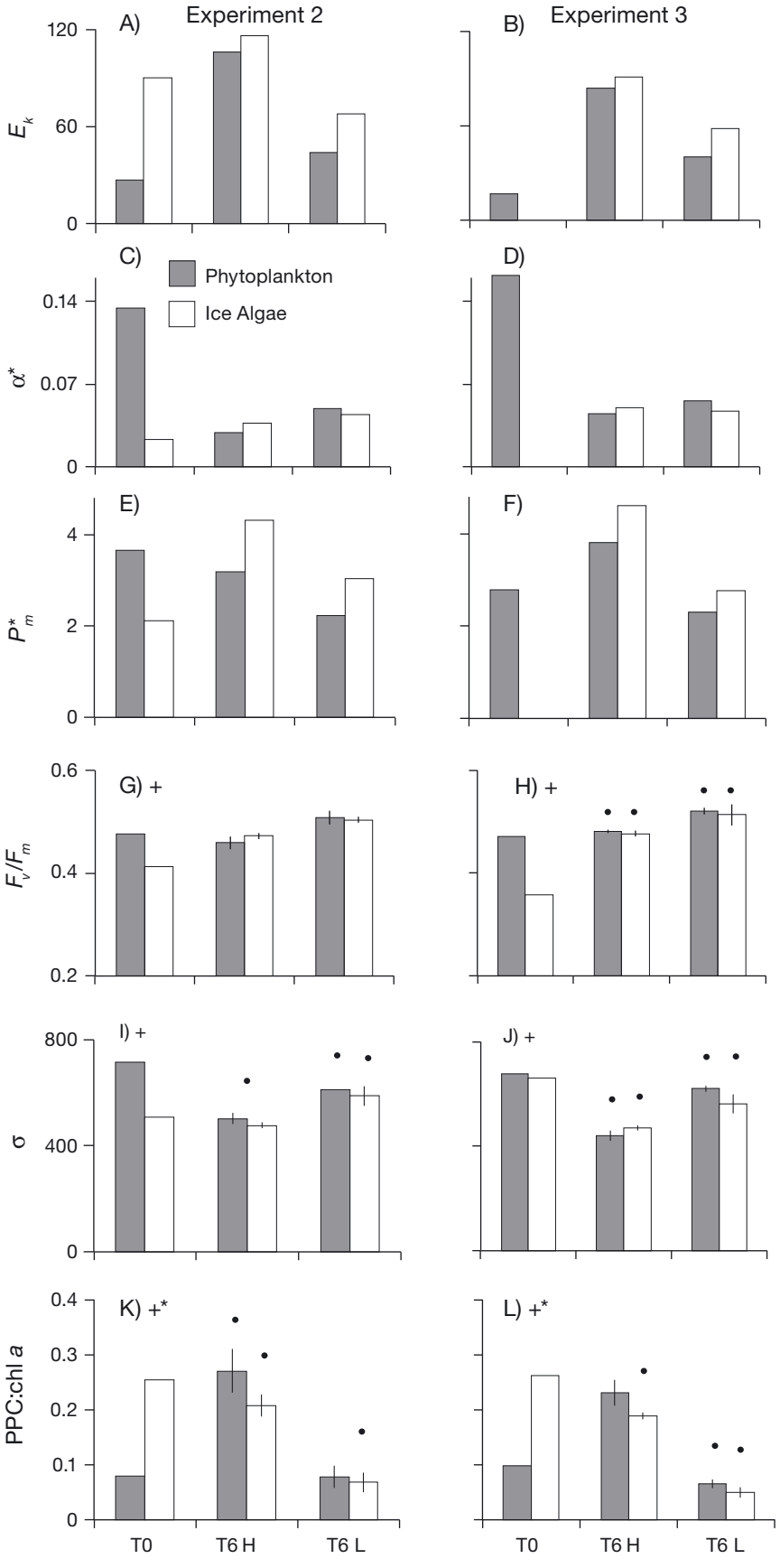

Fig. 6. Photophysiology parameters (mean, with ± SD shown in G–L T6 of ice algae and phytoplankton for Expts 2 and 3 (24 h light) on Day 0 (T0) and Day 6 (T6) incubated under high (H) and low (L) light levels. Other details as in Fig. 5

community composition through settling column experiments. Overall, ice algal communities had consistently higher sinking rates (0.22 ± 0.08 m d^{-1}) than phytoplankton (0.00 ± 0.09 m d^{-1}). Very low sinking rates for phytoplankton persisted over a wide range of settling times (Table 5). For ice algae, the highest sinking rate was observed after 4 h (Stn 58; 1.11 m d^{-1}), compared to those after 24 h (Stn 58; 0.28 m d^{-1}).

The taxonomic composition of the buoyant and sinking communities showed that when *P. antarctica* was present, it made up a disproportionately higher fraction of the settled biomass (estimated from biovolume) than would have been expected from an even distribution of communities throughout the settling column (Fig. 7, Stns 40, 58, 66, and 71). Conversely, pennate diatoms were often buoyant, demonstrated by their low abundance in the settled biomass relative to their expected abundance based on an even distribution. The fate of centric and small, unidentified phytoplankton cells was less clear. These groups were more often found at the top and middle sections of the settling column than the bottom, indicating relatively slow sinking speeds over the length of the experiments (4 to 24 h).

DISCUSSION

Magnitude of spring ice algal blooms

An earlier study of WAP ice ecosystems qualitatively described the slush layer as dark brow-colored ice with slush-filled gaps (Miller & Grobe 1996). Studies on WAP ice ecosystems have either been limited to Marguerite Bay (Massom et al. 2006) or

Table 5. Sinking rates of ice algae from the slush layer and phytoplankton communities from near surface waters (n = 2, 3)

	Station	Mean sinking rate (m d^{-1}, ± SD)
Phytoplankton		
	2	0.06 ± 0.00
	15	0.13 ± 0.03
	38	−0.11 ± 0.02
	40	−0.10 ± 0.06
	44	0.00 ± 0.01
	48	0.03 ± 0.00
Ice algae		
	50	0.17 ± 0.02
	58	0.38 ± 0.69
	62	0.18 ± 0.04
	66	0.24 ± 0.07
	68	0.18 ± 0.04
	71	0.22 ± 0.01
	78	0.17 ± 0.01

conducted outside of our study area, farther south in the Bellingshausen Sea (Boyd et al. 1995, Miller & Grobe 1996, Fritsen et al. 2011). Slush layer ice algal concentrations measured during our study were up to 3 times greater than observed earlier in spring in Marguerite Bay (71 mg m^{-3}; Massom et al. 2006), but integrated values from our study were 3 times lower than those of Massom et al. (2006; 309 mg m^{-2}). Differences were likely due to our thinner (0.39–1.18 m) dispersed ice pack compared to the rafted ice floes up to 10–15 m thick in Massom et al. (2006). Depth-integrated biomass at most stations in our study was between 10 and 100 mg chl *a* m^{-2}, and the majority were in close agreement with estimates from the spring Bellingshausen Sea ASPeCt dataset (25–35 mg chl *a* m^{-2} in Saenz & Arrigo 2014). Our ice biomass estimates are likely conservative because, similar to the challenging sample collection noted by Miller & Grobe (1996) during the ANT-XI/3 expedition, the slush was easily lost or diluted with seawater during collection. In other Antarctic regions, observations of chl *a* within slush layers range from 80–244 mg m^{-2} (reviewed by Arrigo & Thomas 2004), and concentrations as high as 439 mg m^{-3} (Kattner et al. 2004) have been reported. In a metadata analysis of ice communities across the Amundsen and Bellingshausen Seas, Meiners et al. (2012) reported that ice algal biomass was evenly distributed throughout the ice core, with surface (37.1%), interior (29.8%), and bottom habitats (33.2%) contributing almost evenly to depth-integrated chl *a*. These observations agree with our first-ever mid to late spring measurements

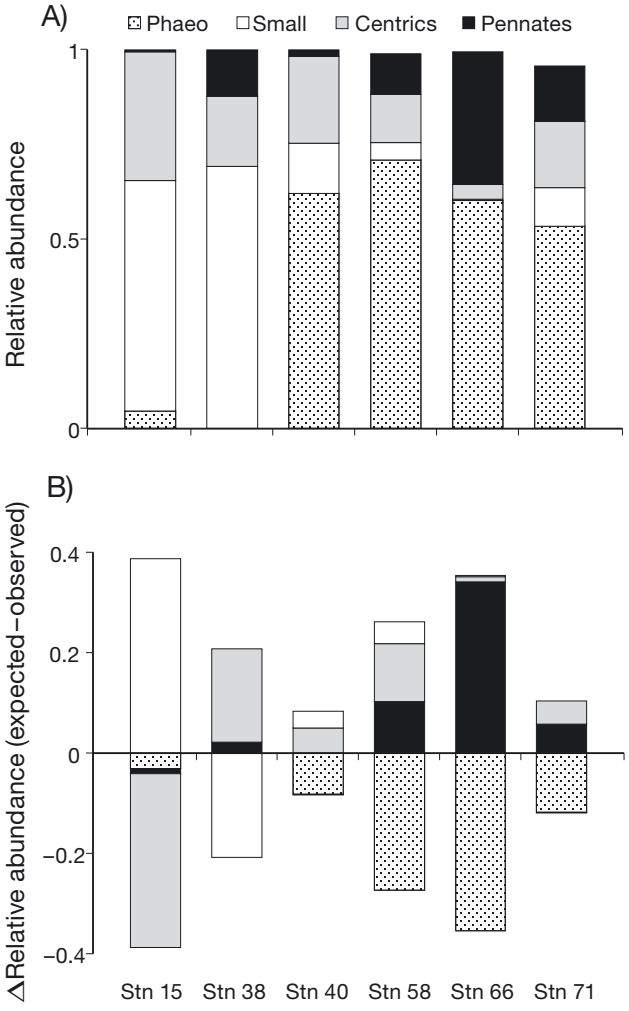

Fig. 7. (A) Taxonomic composition of communities in settling column experiments. (B) Change in relative abundance of taxa in bottom of settling columns from even distribution (expected even distribution − observed distribution of settled biomass): 0 would indicate there was no change from an expected even distribution. >0 indicates taxa were positively buoyant and ascended from the bottom to the middle and top portions of the settling column. <0 indicates taxa were negatively buoyant and sank to the bottom of the settling column. Stn: station (see Fig. 1)

of sea ice algae along the LTER grid showing that elevated chl *a* concentrations were contained in slush layers throughout the sea ice.

Ice algal community physiology and composition

Elevated irradiance and frequent seawater exchange through porous ice are associated with horizontal slush layers (Thomas et al. 1998) and support bloom formation, as indicated by the lower POC:chl *a* (Geider et al. 1997) and POC:PON ratios observed

here and by Kattner et al. (2004). In our sea ice samples, nutrient concentrations were often high, and sometimes equal to or above expected values based on seawater exchange throughout the sea ice. High ice algal productivity has been observed within these slush layers, comparable to that of phytoplankton in other regions (Lizotte & Sullivan 1991), prompting the terms 'biological soup' and 'chemostat in ice' (Thomas et al. 1998). We also observed the highest values for $P_m^\star$ and $\alpha^\star$ in the slush layer, indicating high maximal growth rates. Ice algae in the slush layer must maintain large numbers of PSII reaction centers to sustain the observed high $P_m^\star$ and $\alpha^\star$ with low PSII reaction center efficiencies (F_v/F_m; Murchie & Lawson 2013). These results suggest that slush layers provide a very favorable combination of light and nutrients for growth relative to other ice habitats.

Despite significant differences in photosynthetic parameters ($P_m^\star$ and $\alpha^\star$) between communities living in the slush layer and other habitats of the sea ice, there were no consistent differences in community composition, as *Phaeocystis antarctica* dominated communities throughout the sea ice. High connectivity of porous sea ice and the motility of some phytoplankton, such as the flagellate stage of *P. antarctica,* may explain the absence of algal zonation with respect to community composition throughout sea ice (Syvertsen & Kristiansen 1993). In previous studies, *P. antarctica* has been observed in both single-cell and colonial forms in sea ice, but it has rarely been dominant (Garrison & Buck 1989, Syvertsen & Kristiansen 1993, Arrigo et al. 2003), although Arrigo et al. (2003) observed high *P. antarctica* biomass in newly formed sea ice. Haptophytes, such as *P. antarctica*, have been observed at low relative abundances in infiltration and surface sea ice communities in the Weddell Sea (Syvertsen & Kristiansen 1993) and Eastern Antarctic region (Trevena et al. 2000) and in bottom ice communities in the Bellingshausen Sea (Fritsen et al. 2011). More often, pennate diatoms such as *Nitzschia* (Garrison & Buck 1989, Syvertsen & Kristiansen 1993, Thomas et al. 1998), *Amphiprora* (Thomas et al. 1998, Guglielmo et al. 2000), and *Fragilariopsis* (Thomas et al. 1998) dominated slush layers and other habitats in the sea ice.

The dominance of colonial *P. antarctica* blooms we observed in slush layers has the potential to influence upper trophic levels, particularly along the WAP. In other regions of the Antarctic, swarms of juvenile krill removed 3 to 4 cm of ice algal layers from the slush community within 30 min (Syvertsen & Kristiansen 1993), suggesting that these layers can be a rich food source for krill. However, other field and laboratory studies have shown that krill (*Euphausia superba*) do not readily graze *P. antarctica* (Haberman et al. 2002), especially in colonial form (Haberman et al. 1993). Krill prefer to feed on diatoms, such as the common ice genus *Nitzschia*, as suggested by selective grazing experiments that showed higher grazing rates on diatoms (Haberman et al. 2003). The mucus matrix of *P. antarctica* may clog the feeding apparatus of zooplankton (Schnack 1985) or prevent ingestion (Hansen et al. 1994). Interestingly, we only observed swarms of krill feeding in the slush layer at the northern-most ice station (Stn 24, Expt 1), which was one of the few ice stations dominated by diatoms. Massom et al. (2006) found that despite heavy ice conditions and high ice algal biomass in slush layers, krill recruitment was low along the WAP, although no phytoplankton taxonomic information was available in that study. These findings, paired with our anecdotal field observations, hint at the potential roles that the physical structure of the sea ice may play in shaping lower and upper trophic level dynamics of the ocean ecosystem.

Ice algal and phytoplankton community responses to simulated ice melt

Prior to simulated melt out, ice algal communities within the sea ice were acclimated (E_k) to light levels representative of mid to late spring MLs in the Southern Ocean (Smith & van Hilst 2003) and those defined as low light conditions in our growth experiments (90 µmol photon m^{-2} s^{-1}). These levels of light acclimation are similar to those measured previously in ice algal communities near Palmer Station during late spring (>80 µmol photon m^{-2} s^{-1}; Prezelin et al. 1998). Therefore, our low light treatments simulated the transition of ice algal communities from the sea ice to the water column under mid to late spring ML conditions. High light treatments simulated the transition of ice algal communities from the sea ice to the water column under higher light conditions representative of stratified summer ML conditions (Smith & van Hilst 2003, Mills et al. 2010).

In contrast to ice algae, phytoplankton beneath sea ice in our study were acclimated to much lower light levels (17 to 47 µmol photon m^{-2} s^{-1}) prior to growth experiment incubations. Therefore, growth experiments simulate phytoplankton transitioning from a deeply mixed low light environment beneath the sea ice to ice-free waters with a spring ML (low light treatment) and a summer ML (high light treatment).

Photoacclimation of *P. antarctica* and diatoms

The initial phytoplankton and ice algal communities in our experiments were dominated by chain-forming diatoms, a well-documented bloom-forming group across the WAP (Prezelin et al. 2000, Garibotti et al. 2003a,b) and colonial *P. antarctica*. These taxa are thought to employ different adaptive strategies to variable (Van Leeuwe & Stefels 2007, Mills et al. 2010) and stable (Moisan et al. 1998, Van Leeuwe & Stefels 1998, Moisan & Mitchell 1999, Arrigo et al. 2010) light conditions that persist during the spring transition period. Cullen & MacIntyre (1998) proposed the terms 'mixers' and 'layer-formers' to describe phytoplankton adapted to a variable light field under mixing conditions and a stable light field under stratified conditions, respectively. Field and laboratory studies have identified *P. antarctica* as a mixer based on its ability to utilize the maximum, rather than the average, irradiance experienced in the water column (Mills et al. 2010) and its observed dominance in blooms that form in deeply mixed conditions of the Ross Sea (Arrigo et al. 1999, 2010). Conversely, the diatom *Fragilaropsis cylindrus* was suggested to be more of a layer-former, adapted to higher and less variable light (Arrigo et al. 2010, Mills et al. 2010).

In the 12:12 h growth experiment (Expt 1), phytoplankton chl *a* and POC-based growth rates were higher than those of ice algae, suggesting that under these light conditions, phytoplankton growth would outpace ice algal growth when released from the ice into the water column. Despite the dominance of diatoms at T6 in the Expt 1 phytoplankton communities, *P. antarctica* increased and diatoms decreased in relative abundance over the 6 d experiment, suggesting that *P. antarctica* has a competitive advantage over diatoms in both high and low light conditions. Similarly, in the high and low light ice algal communities, *P. antarctica* increased in abundance relative to diatoms, and in this instance, was the dominant taxon by T6. Arrigo et al. (2010) and Mills et al. (2010) showed that *P. antarctica* growth rates exceeded those of the diatom species *F. cylindrus* at irradiances <250 µmol photon m^{-2} s^{-1}. These light levels are within the range of our study, which simulates spring (low light) and summer (high light) mixed layer depth (MLD) scenarios. Comparison of mixed community (*P. antarctica*–diatoms) photoacclimation at T6 from our study (Expt 1, 12:12 h) showed that communities with higher proportions of *P. antarctica* had higher maximum photosynthesis rates in high light. This result is in agreement with others (Arrigo et al. 2010, Mills et al. 2010) showing that under high light, *P. antarctica* maximizes its growth potential rather than optimizing energy capture and utilization.

If cells capture energy faster than they can process it, the excess energy can damage reaction centers within the photosystem, which slows growth (Long et al. 1994). Taxonomically mixed communities (Expt 1, 12:12 h) with a greater proportion of *P. antarctica* had lower values for F_v/F_m, potentially indicative of damaged photosystems. Alternatively, community differences in F_v/F_m may be a result of the different photoprotective strategies employed by diatoms and *P. antarctica*. Laboratory studies show that both *P. antarctica* and diatoms employ rapid xanthophyll cycling to dissipate excess energy as heat and protect the reaction center from photodamage (Moisan et al. 1998, Van Leeuwe & Stefels 2007, Kropuenske et al. 2009); however, comparative studies have suggested this is a dominant photophysiology strategy in diatoms, but not *P. antarctica* (Kropuenske et al. 2009, Arrigo et al. 2010, Van de Poll et al. 2011). Rather, *P. antarctica* invests in the slower photoacclimation mechanism of D1 protein repair following photodamage (Kropuenske et al. 2009). While *P. antarctica* may be more susceptible to photodamage, as suggested by Kropuenske et al. (2009) and Mills et al. (2010), *P. antarctica* increased in relative abundance in all experiments. These results suggest that both ice-derived and non-ice-derived *P. antarctica* were able to compensate for any photodamage incurred and have the potential to outcompete other taxa under high and low light conditions.

Variability within *P. antarctica*-dominated communities

Our growth experiments suggest that light history can also affect the response of ice algal or phytoplankton communities dominated by *P. antarctica* to changes in the light environment. In Expts 2 and 3, ice algal growth rates were higher than those of phytoplankton, suggesting that ice algal seeding and subsequent growth would outpace that of phytoplankton growth. PvE parameters indicate that phytoplankton were initially acclimated to lower light levels than ice algae. Our results from the growth experiments suggested that deeply mixed under-ice phytoplankton communities (E_k: 17 to 24 µmol photon m^2 s^{-1}) experience a 5-fold increase in light when transitioning to a mid to late spring ML (low light condition; 91 ± 25 µmol photon m^{-2} s^{-1}). In contrast, the light environment experienced by ice

algal communities transitioning from sea ice to a deeply mixed open-water environment (low light) remains unchanged. At T6, ice algae remained acclimated to higher light levels, driven by their higher P^*_m and growth rates than phytoplankton. Phytoplankton employed higher photoprotective pigment to chl *a* ratios (PPC:chl *a*) than ice algae in order to adjust to the order of magnitude increase in their light environment. While light history affected carbon fixation and photoprotective pigment composition, it appeared to have no effect on F_v/F_m or σ_{PSII} in either sea ice or phytoplankton communities. Others have noted that species composition, rather than environment, often controls the variability observed in PSII parameters (Moore et al. 2005, 2006). Our results suggest that light history has a lasting effect on photoacclimation parameters, including carbon fixation and pigment composition, but not on the potentially community composition-driven PSII parameters in *P. antarctica*-dominant communities.

The contrasting light environments of the ice and water column may support the variety of *P. antarctica* populations we observed along the coastal WAP in spring. Gäbler-Schwarz et al. (2015) found that within Antarctic regions, bloom-forming *P. antarctica* were genetically diverse and distinctly different across regions (e.g. Ross Sea, Antarctic Circumpolar Current, Antarctic Peninsula). They also found that geographically close, rather than genetically close, isolates responded similarly to environmental changes, further suggesting that environmental conditions of the ice or the water column in spring may influence population responses post-ice melt.

P. antarctica along the WAP

Our experimental results suggest that, while colonial *P. antarctica* communities from the sea ice and the water column vary in their immediate responses to changes in their light environment, they have the potential to increase in abundance relative to other taxa and dominate the community within a week of acclimation. However, their success in utilizing resources may be balanced by their rate of sinking relative to other taxa, especially in stratified conditions. We observed that, when present, *P. antarctica* made up a larger fraction of the sinking community than diatoms (neutral or positively buoyant), suggesting that *P. antarctica* colonies have higher sinking rates than other taxa. Others have also reported rapid export of *P. antarctica* blooms (DiTullio et al. 2000) and *P. antarctica–Nitzschia* ice algal aggregates (Riebesell et al. 1991). However, Riebesell et al. (1991) noted that ice algae from the slush layer, relative to other ice habitats, did not form aggregates and had lower sinking rates. Additionally, Becquevort & Smith (2001) observed that diatoms and dinoflagellates had higher sinking rates than *P. antarctica*. The sinking and export rates of *P. antarctica* relative to other taxa remain unclear, and may be related to their respective metabolic activity (Waite et al. 1997) or cell density (Peperzak et al. 2003), both of which are beyond the scope of this study. Our data suggest that ice algal communities have faster sinking rates than phytoplankton communities, and that *P. antarctica* from both the ice and the water column sink disproportionately more than other taxa along the WAP. The absolute magnitudes of sinking rates measured in this study are likely underestimates, as indicated by the error associated with sinking rates calculated after <24 h (higher sinking rates) and 24 h (lower sinking rates), as discussed by Bienfang (1981).

Studies suggest that colonial *P. antarctica* can be prevalent in sea ice and is sometimes dominant, co-occurring in late spring with diatoms in coastal surface waters of the Bellingshausen Sea (Savidge et al. 1995), Gerlache Strait (Rodriguez et al. 2002, Varela et al. 2002), and the WAP (Arrigo et al. 2017, this study). However, dominance of *P. antarctica* may be a spring phenomenon, because this dominance does not persist into summer phytoplankton blooms recorded in long-term data sets along the WAP. Garibotti et al. (2003b) suggested that the seasonal succession of phytoplankton is tied to the timing of ice retreat where near-shore phytoplankton blooms associated with the ice edge are diatom-dominated. *P. antarctica* is often present, but not dominant, in these early summer communities (Rodriguez et al. 2002, Varela et al. 2002, Garibotti et al. 2003b, Annett et al. 2010). Observations of higher *P. antarctica* concentrations are generally limited to near-shore regions such as Marguerite Bay (Garibotti et al. 2003b, Kozlowski et al. 2011) or Bransfield Strait (Trimborn et al. 2015). Following the diatom bloom, Garibotti et al. (2003b, 2005) suggested that communities shift to dominance by small unidentified flagellates and then by cryptophytes.

Elevated irradiance along the WAP in summer could explain the shift from either mixed or *P. antarctica*-dominated communities in spring to observed diatom dominance in summer (Garibotti et al. 2003b, 2005). Culture studies show that the diatom *F. cylindrus* has a competitive advantage when grown under irradiances corresponding to a 7 m MLD (Mills et al.

2010), irradiances generally greater than those in our study. In spring, deep MLDs (60 m) at Palmer Station (Ducklow et al. 2012) and across the WAP create low light conditions and are potentially conducive to higher *P. antarctica* abundance, as observed in northern Marguerite Bay (Rozema et al. 2017) and the WAP (Arrigo et al. 2017), but not further north at Palmer Station (Schofield et al. 2017). Typically in coastal waters (<50 km from shore) in mid-December, the water column abruptly shifts from unstable to stratified (MLD of 10 to 15 m) conditions, creating a high and stable light environment, which potentially favors the diatom-dominated blooms seen by Rozema et al. (2017) and observed in summer stratified conditions (Garibotti et al. 2003b, Garibotti et al. 2005, Annett et al. 2010, Ducklow et al. 2012). The onset of stratification and, consequently, the potential for nutrient limitation and photoinhibition, make sinking losses a more important component of total loss processes for phytoplankton populations (Cullen & MacIntyre 1998). The combination of the lower growth rate of *P. antarctica* at high irradiance (Mills et al. 2010) and higher sinking rates than diatoms (this study) may explain the nearly ubiquitous absence of *P. antarctica* dominance along the coastal WAP in summer phytoplankton blooms. In contrast to highly stratified coastal waters, mid and outer continental shelf and offshore waters have deeper MLs (Prezelin et al. 2000, Martinson et al. 2008, Vernet et al. 2008) Recent studies have observed that *P. antarctica* can comprise ≥50% of the phytoplankton community in offshore waters in spring (Arrigo et al. 2017) and that these high relative abundances can persist into summer (Kozlowksi et al. 2011, Trimborn et al. 2015).

The combination of field survey and experimental results suggest that sea ice is a potential source of *P. antarctica* to the water column, and that these ice-derived *P. antarctica* are viable under light conditions phytoplankton would experience from late spring through summer. A complementary study (Arrigo et al. 2017) found that *P. antarctica* distributions in the phytoplankton were positively correlated with ice cover, further suggesting that the *P. antarctica* blooms in sea ice may seed the water column. The ability of *P. antarctica* to grow faster at low light levels (Kropuenske et al. 2009) and increase in abundance relative to other taxa (this study), may allow it to maintain its dominance through the ice-covered spring season, contributing to moderate spring phytoplankton blooms in variable sea ice cover (Arrigo et al. 2017). Potential coupling between the sea ice and ocean communities along the WAP has been suggested by similar qualitative observations by Massom et al. (2006), who described large-scale intra-ice pack spring phytoplankton blooms associated with high biomass slush layers in the sea ice.

CONCLUSIONS

The WAP sea ice experiences enhanced and widespread surface flooding during late spring, leading to pronounced slush ice algal communities that are dominated by the bloom-forming colonial haptophyte *P. antarctica.* During spring, the ice algal and phytoplankton communities are highly interconnected, as suggested by their taxonomic composition. Our ship-board experiments suggest that ice algae, especially *P. antarctica,* from slush layers can contribute to phytoplankton communities during sea ice melt. This ice–ocean coupling along the WAP is likely driven by high rates of flooding and seawater exchange in spring. Sea ice and water column populations of *P. antarctica* may give this taxon a unique advantage for dominance by having multiple seed populations adapted to different light regimes. However, this contribution may be limited due to *P. antarctica's* enhanced sinking potential relative to other taxa. Ice algal biomass location (slush, surface, interior, or bottom layer), taxonomic composition, and its role in seeding phytoplankton blooms may have broader consequences for upper trophic levels. Furthermore, as the WAP experiences continued warming, the role sea ice plays in controlling light availability and stratification may alter the structure of phytoplankton blooms, particularly for *P. antarctica.*

Acknowledgements. We acknowledge the Captain and crew of the RV 'Nathaniel B. Palmer.' We also thank Gert L. van Dijken and Matt M. Mills for their advice throughout the course of the project. Funding was provided by the Polar Programs – National Science Foundation grant to K.R.A. (Grant no. ANT-1063592).

LITERATURE CITED

Ackley SF, Sullivan CW (1994) Physical controls on the development and characteristics of Antarctic sea ice biological communities — a review and synthesis. Deep Sea Res I 41:1583–1604

Ackley SF, Lewis MJ, Fritsen CH, Xie H (2008) Internal melting in Antarctic sea ice: development of 'gap layers'. Geophys Res Lett 35:L11503

Álvarez E, López-Urrutia Á, Nogueira E (2012) Improvement of plankton biovolume estimates derived from

image-based automatic sampling devices: application to FlowCAM. J Plankton Res 34:454–469
Annett AL, Carson DS, Crosta X, Clarke A, Ganeshram RS (2010) Seasonal progression of diatom assemblages in surface waters of Ryder Bay, Antarctica. Polar Biol 33:13–29
Arrigo KR, Thomas DN (2004) Large-scale importance of sea ice biology in the Southern Ocean. Antarct Sci 16: 471–486
Arrigo KR, Robinson DH, Worthen DL, Dunbar RB, DiTullio GR, VanWoert M, Lizotte M (1999) Phytoplankton community structure and the drawdown of nutrients and CO_2 in the Southern Ocean. Science 283:365–367
Arrigo KR, Robinson DH, Dunbar RB, Leventer AR, Lizotte MP (2003) Physical control of chlorophyll *a*, POC, and TPN distributions in the pack ice of the Ross Sea, Antarctica. J Geophys Res 108:3316–3339
Arrigo KR, Mills MM, Kropuenske LR, Van Dijken GL, Alderkamp AC, Robinson DH (2010) Photophysiology in two major southern ocean phytoplankton taxa: photosynthesis and growth of *Phaeocystis antarctica* and *Fragilariopsis cylindrus* under different irradiance levels. Integr Comp Biol 50:950–966
Arrigo KR, Van Dijken GL, Alderkamp AC, Erikson ZK and others (2017) Early spring phytoplankton dynamics in the western Antarctic Peninsula. J Geophys Res Oceans 122
Becquevort S, Smith WO (2001) Aggregation, sedimentation and biodegradability of phytoplankton-derived material during spring in the Ross Sea, Antarctica. Deep Sea Res II 48:4155–4178
Bernard KS, Steinberg DK, Schofield OME (2012) Summertime grazing impact of dominant macrozooplankton off the western Antarctic Peninsula. Deep-Sea Res A Oceanogr Res Pap 62:111–122
Bienfang PK (1981) SETCOL — a technologically simple and reliable method for measuring phytoplankton sinking rates. Can J Fish Aquat Sci 38:1289–1294
Boyd PW, Robinson C, Savidge G, Le B, Williams PJ (1995) Water column and sea-ice primary production during Austral spring in the Bellingshausen Sea. Deep Sea Res II 42:1177–1200
Cullen JJ, Davis RF (2003) The blank can make a big difference in oceanographic measurements. Limnol Oceanogr Bull 12:29–35
Cullen JJ, MacIntyre JG (1998) Behavior, physiology, and the niche of depth-regulating phytoplankton. In: Anderson DM, Cembella AD, Hallegraeff GM (eds) Physiological ecology of harmful algal blooms. Springer-Verlag, Berlin p 559–580
Daly KL (1990) Overwintering development, growth, and feeding of larval *Euphausia superba* in the Antarctic marginal ice zone. Limnol Oceanogr 35:1564–1576
Daly KL, Macaulay MC (1988) Abundance and distribution of krill in the ice edge zone of the Weddell Sea, austral spring 1983. Deep-Sea Res A Oceanogr Res Pap 35:21–41
DiTullio GR, Grebmeier JM, Arrigo KR, Lizotte MP and others (2000) Rapid and early export of *Phaeocystis antarctica* blooms in the Ross Sea, Antarctica. Nature 404:595–598
Ducklow HW, Baker K, Martinson DG, Quetin LB and others (2007) Marine pelagic ecosystems: the West Antarctic Peninsula. Philos Trans R Soc Lond B Biol Sci 362:67–94
Ducklow HW, Clarke A, Dickhut R, Doney SC and others (2012) The marine system of the Antarctic Peninsula. In: Rogers AD, Johnston NM, Murphy EJ, Clarke A (eds) Antarctic ecosystems: an extreme environment in a changing world. Blackwell Publishing, Chichester, p 121–159
Ducklow HW, Fraser WR, Meredith MP, Stammerjohn SE and others (2013) West Antarctic Peninsula: an ice-dependent coastal marine ecosystem in transition. Oceanography 26:190–203
Fritsen CH, Ackley SF, Kremer JN, Sullivan CW (1998) Flood-freeze cycles and microalgal dynamics in Antarctic pack ice. Antarct Res Ser 73:1–21
Fritsen CH, Coale S, Neenan D, Gibson A, Garrison D (2001) Biomass, production and microhabitat characteristics near the freeboard of ice floes in the Ross Sea, Antarctica, during the austral summer. Ann Glaciol 33:280–286
Fritsen CH, Wirthlin ED, Momberg DK, Lewis MJ, Ackley SF (2011) Bio-optical properties of Antarctic pack ice in the early austral spring. Deep Sea Res II 58:1052–1061
Gäbler-Schwarz S, Medlin LK, Leese F (2015) A puzzle with many pieces: the genetic structure and diversity of *Phaeocystis antarctica* Karsten (Prymnesiophyta). Eur J Phycol 50:112–124
Garibotti IA, Vernet M, Kozlowski WA, Ferrario ME (2003a) Composition and biomass of phytoplankton assemblages in coastal Antarctic waters: a comparison of chemotaxonomic and microscopic analyses. Mar Ecol Prog Ser 247:27–42
Garibotti IA, Vernet M, Ferrario ME, Smith RC, Ross RM, Quetin LB (2003b) Phytoplankton spatial distribution patterns along the western Antarctic Peninsula (Southern Ocean). Mar Ecol Prog Ser 261:21–39
Garibotti IA, Vernet M, Ferrario M (2005) Annually recurrent phytoplanktonic assemblages during summer in the seasonal ice zone west of the Antarctic Peninsula (Southern Ocean). Deep Sea Res I 52:1823–1841
Garrison DL, Buck KR (1989) The biota of the Antarctic pack ice in the Weddell Sea and Antarctic Peninsula regions. Polar Biol 10:211–219
Garrison DL, Buck KR, Fryxell GA (1987) Algal assemblages in Antarctic pack ice and in ice-edge plankton. J Phycol 23:564–572
Geider RJ, MacIntyre HL, Kana TM (1997) Dynamic model of phytoplankton growth and acclimation: responses of the balanced growth rate and chlorophyll *a*:carbon ratio to light, nutrient-limitation and temperature. Mar Ecol Prog Ser 148:187–200
Guglielmo L, Carrada GC, Catalano G, Dell'Anno A and others (2000) Structural and functional properties of sympagic communities in the annual sea ice at Terra Nova Bay (Ross Sea, Antarctica). Polar Biol 23:137–146
Haberman KL, Ross RM, Quetin LB (1993) Palmer LTER: grazing by the Antarctic krill *Euphausia superba* on *Nitzschia* sp. and *Phaeocystis* sp. monocultures. Antarct J US 28:217–219
Haberman KL, Ross RM, Quetin LB, Vernet M, Nevitt GA, Kozlowski W (2002) Grazing by Antarctic krill *Euphausia superba* on *Phaeocystis antarctica*: an immunochemical approach. Mar Ecol Prog Ser 241:139–149
Haberman KL, Ross RM, Quetin LB (2003) Diet of the Antarctic krill (*Euphausia superba* Dana). II. Selective grazing in mixed phytoplankton assemblages. J Exp Mar Biol Ecol 283:97–113
Hansen B, Verity P, Falkenhaug T, Tande KS, Norrbin F (1994) On the trophic fate of *Phaeocystis pouchetti* (Harriot). V. Trophic relationships between *Phaeocystis* and

zooplankton: an assessment of methods and size dependence. J Plankton Res 16:487–511
Holm-Hansen O, Lorenzen CJ, Holmes RW, Strickland JDH (1965) Fluorometric determination of chlorophyll. ICES J Mar Sci 30:3–15
Jakobsen HH, Carstensen J (2011) FlowCAM: sizing cells and understanding the impact of size distributions on biovolume of planktonic community structure. Aquat Microb Ecol 65:75–87
Jeffries MO, Morris K, Weeks WF, Worby AP (1997) Seasonal variations in the properties and structural composition of sea ice and snow cover in the Bellingshausen and Amundsen Seas, Antarctica. J Glaciol 43:138–151
Johnson TO, Smith WO Jr (1986) Sinking rates of phytoplankton assemblages in the Weddell Sea marginal ice zone. Mar Ecol Prog Ser 33:131–137
Kattner G, Thomas DN, Haas C, Kennedy H, Dieckmann GS (2004) Surface ice and gap layers in Antarctic sea ice: highly productive habitats. Mar Ecol Prog Ser 277:1–12
Kolber ZS, Ondřej P, Falkowski PG (1998) Measurements of variable chlorophyll fluorescence using fast repetition rate techniques: defining methodology and experimental protocols. Biochim Biophys Acta 1367:88–106
Kottmeier ST, McGrath Grossi S, Sullivan CW (1987) Sea ice microbial communities. VIII. Bacterial production in annual sea ice of McMurdo Sound, Antarctica. Mar Ecol Prog Ser 35:175–186
Kozlowski WA, Deutschman D, Garibotti I, Trees C, Vernet M (2011) An evaluation of the application of CHEMTAX to Antarctic coastal pigment data. Deep-Sea Res I 58:350–368
Kropuenske LR, Mills MM, Van Dijken GL, Bailey S, Robinson DH, Welschmeyer NA, Arrigo KR (2009) Photophysiology in two major Southern Ocean phytoplankton taxa: photoprotection in *Phaeocystis antarctica* and *Fragilariopsis cylindrus*. Limnol Oceanogr 54:1176–1196
Lannuzel D, Schoemann V, Dumont I, Content M and others (2013) Effect of melting Antarctic sea ice on the fate of microbial communities studied in microcosms. Polar Biol 36:1483–1497
Lewis MR, Smith JC (1983) A small volume, short-incubation-time method for measurement of photosynthesis as a function of incident irradiance. Mar Ecol Prog Ser 13:99–102
Liu J, Curry JA, Martinson DG (2004) Interpretation of recent Antarctic sea ice variability. Geophys Res Lett 31:L02205
Lizotte MP, Sullivan CW (1991) Photosynthesis-irradiance relationships in microalgae associated with Antarctic pack ice: evidence for in situ activity. Mar Ecol Prog Ser 71:175–184
Loeb V, Siegel V, Holm-Hansen O, Hewitt R, Fraser W, Trivelpiece W, Trivelpiece S (1997) Effects of sea-ice extent and krill or salp dominance on the Antarctic food web. Nature 387:897–900
Long SP, Humphries S, Falkowski PG (1994) Photoinhibition of photosynthesis in nature. Annu Rev Plant Physiol Plant Mol Biol 45:633–662
Mackey MD, Mackey DJ, Higgins HW, Wright SW (1996) CHEMTAX — a program for estimating class abundances from chemical markers: application to HPLC measurements of phytoplankton. Mar Ecol Prog Ser 144:265–283
Mangoni O, Saggiomo M, Modigh M, Catalano G, Zingone A, Saggiomo V (2009) The role of platelet ice microalgae in seeding phytoplankton blooms in Terra Nova Bay (Ross Sea, Antarctica): a mesocosm experiment. Polar Biol 32:311–323
Marschall HP (1988) The overwintering strategy of Antarctic krill under the pack-ice of the Weddell Sea. Polar Biol 9:129–135
Marshall GJ, Lagun V, Lachlan-Cope TA (2002) Changes in Antarctic Peninsula tropospheric temperatures from 1956 to 1999: a synthesis of observations and reanalysis data. Int J Climatol 22:291–310
Martinson DG, Stammerjohn SE, Smith RC, Iannuzzi RA (2008) Palmer, Antarctica, Long-Term Ecological Research program first 12 years: physical oceanography, spatio-temporal variability. Deep Sea Res II 55:1964–1987
Massom RA, Stammerjohn SE (2010) Antarctic sea ice change and variability — physical and ecological implications. Polar Sci 4:149–186
Massom RA, Eicken H, Haas C, Jeffries MO and others (2001) Snow on Antarctic sea ice. Rev Geophys 39:413–445
Massom RA, Stammerjohn SE, Smith RC, Pook MJ and others (2006) Extreme anomalous atmospheric circulation and its west Antarctic peninsula region in austral spring and summer 2001/02, and its profound impact on sea ice and biota. J Clim 19:3544–3571
Mathot S, Smith WO, Carlson C, Garrison DL, Gowing MM, Vickers CL (2000) Carbon partitioning within *Phaeocystis antarctica* (Prymnesiophyceae) colonies in the Ross Sea, Antarctica. J Phycol 36:1049–1056
Maxwell K, Johnson GN (2000) Chlorophyll fluorescence — a practical guide. J Exp Bot 51:659–668
Meiners KM, Vancoppenolle M, Thanassekos S, Dieckmann GS and others (2012) Chlorophyll *a* in Antarctic sea ice from historical ice core data. Geophys Res Lett 39:L21602
Menden-Deuer S, Lessard EJ (2000) Carbon to volume relationships for dinoflagellates, diatoms, and other protist plankton. Limnol Oceanogr 45:569–579
Meredith MP, King JC (2005) Rapid climate change in the ocean west of the Antarctic Peninsula during the second half of the 20th century. Geophys Res Lett 32:L19604
Miller H, Grobe H (1996) Die Expedition ANTARKTIS-XI/3 mit FS 'Polarstern' 1994, (The expedition ANTARKTIS-XI/3 of RV 'Polarstern' in 1994). Ber Polarforsch 188:1–115
Mills MM, Kropuenske LR, Van Dijken GL, Alderkamp AC and others (2010) Photophysiology in two Southern Ocean phytoplankton taxa: *Phaeocystis antarctica* (Prymnesiophyceae) and *Fragilariopsis cylindrus* (Bacillariophyceae) under simulated mixed-layer irradiance. J Phycol 46:1114–1127
Moisan TA, Mitchell BG (1999) Photophysiological acclimation of *Phaeocystis antarctica* Karsten under light limitation. Limnol Oceanogr 44:247–258
Moisan TA, Olaizola M, Mitchell BG (1998) Xanthophyll cycling in *Phaeocystis antarctica*: changes in cellular fluorescence. Mar Ecol Prog Ser 169:113–121
Montes-Hugo M, Vernet M, Martinson D, Smith R, Iannuzzi R (2008) Variability on phytoplankton size structure in the western Antarctic Peninsula (1997-2006). Deep Sea Res II 55:2106–2117
Montes-Hugo M, Doney SC, Ducklow HW, Fraser W, Martinson D, Stammerjohn SE, Schofield O (2009) Recent changes in phytoplankton communities associated with rapid regional climate change along the western Antarctic Peninsula. Science 323:1470–1473
Moore CM, Lucas MI, Sanders R, Davidson R (2005) Basin-scale variability of phytoplankton bio-optical characteris-

tics in relation to bloom state and community structure in the Northeast Atlantic. Deep Sea Res I 52:401–419

Moore CM, Suggett DJ, Hickman AE, Kim YN and others (2006) Phytoplankton accumulation and photoadaptation response to environmental gradients in a shelf sea. Limnol Oceanogr 51:936–949

Murchie EH, Lawson T (2013) Chlorophyll fluorescence analysis: a guide to good practices and understanding some new applications. J Exp Bot 64:3983–3998

Peperzak L, Colijn F, Koeman R, Gieskes WWC, Joordens JCA (2003) Phytoplankton sinking rates in the Rhine region of freshwater influence. J Plankton Res 25:365–383

Perovich DK, Elder BC, Claffey KJ, Stammerjohn S and others (2004) Winter sea-ice properties in Marguerite Bay, Antarctica. Deep Sea Res II 51:2023–2039

Platt T, Gallegos CL, Harrison WG (1980) Photoinhibition of photosynthesis in natural assemblages of marine phytoplankton. J Mar Res 38:687–701

Prezelin BB, Moline MA, Matlick HA (1998) Icecolors 1993: spectral UV radiation effects on Antarctic frazil ice algae. In: Lizotte MP, Arrigo KR (eds) Antarctic sea ice: biological processes, interactions and variability. Antarctic Research Series Vol 73. American Geophysical Union, Washington, DC, p 45–83

Prezelin BB, Hofmann EE, Mengelt C, Klink JM (2000) The linkage between upper circumpolar deepwater (UCDW) and phytoplankton assemblages on the west Antarctic Peninsula continental shelf. J Mar Res 58:165–202

Riebesell U, Schloss I, Smetacek V (1991) Aggregation of algae released from melting sea ice: implications for seeding and sedimentation. Polar Biol 11:239–248

Rodriguez F, Varel M, Zapata M (2002) Phytoplankton assemblages in the Gerlache and Bransfield Straits (Antarctic Peninsula) determined by light microscopy and CHEMTAX analysis of HPLC pigment data. Deep Sea Res II 49:723–747

Ross RM, Quetin LB, Martinson DG, Iannuzzi RA, Stammerjohn SE, Smith RC (2008) Palmer LTER: patterns of distribution of five dominant zooplankton species in the epipelagic zone west of the Antarctic Peninsula, 1993–2004. Deep Sea Res II 55:2086–2105

Ross RM, Quetin LB, Newberger T, Shaw CT, Jones JL, Oakes SA, Moore KJ (2014) Trends, cycles, interannual variability for three pelagic species west of the Antarctic Peninsula 1993–2008. Mar Ecol Prog Ser 515:11–32

Rozema PD, Venables HJ, Van de Poll WH, Clarke A, Meredith MP, Buma AGJ (2017) Interannual variability in phytoplankton biomass and species composition in northern Marguerite Bay (West Antarctic Peninsula) is governed by both winter sea ice cover and summer stratification. Limnol Oceanogr 62:235–252

Saenz BT, Arrigo KR (2014) Annual primary production in Antarctic sea ice during 2005–2006 from a sea ice state estimate. J Geophys Res Oceans 119:3645–3678

Savidge G, Harbour D, Gilpin LC, Boyd PW (1995) Phytoplankton distributions and production in the Bellingshausen Sea, Austral spring 1992. Deep Sea Res II 42:1201–1224

Schnack SB (1985) Feeding by *Euphausia superba* and copepod species in response to varying concentrations of phytoplankton. In: Siegfried WR, Condy PR, Laws RM (eds) Antarctic nutrient cycles and food webs. Springer Verlag, Berlin and Heidelberg, p 311–323

Schofield O, Saba G, Coleman K, Carvalho F and others (2017) Decadal variability in coastal phytoplankton community composition in a changing West Antarctic Peninsula. Deep-Sea Res I 124:42–54

Smith WO, van Hilst CM (2003) Effects of assemblage composition on the temporal dynamics of carbon and nitrogen uptake in the Ross Sea. In: DiTullio GR, Dunbar RB (eds) Biogeochemistry of the Ross Sea. Antarctic Research Series Vol 78. American Geophysical Union, Washington, DC, p 197–208

Stammerjohn SE, Martinson DG, Smith RC, Iannuzzi RA (2008) Sea ice in the western Antarctic Peninsula region: spatial-temporal variability from ecological and climate change perspectives. Deep Sea Res II 55: 2041–2058

Steinberg DK, Ruck KE, Gleiber MR, Garzio LM and others (2015) Long term (1993-2013) changes in macrozooplankton off the Western Antarctic Peninsula. Deep Sea Res I 101:54–70

Syvertsen EE, Kristiansen S (1993) Ice algae during EPOS, leg 1: assemblages, biomass, origin, and nutrients. Polar Biol 13:61–65

Thomas DN, Lara JN, Haas C, Schnack-Schiel SB and others (1998) Biological soup within decaying summer sea ice in the Amundsen Sea, Antarctica. Antarct Res Ser 73:161–171

Timco GW, Frederking RMW (1996) A review of sea ice density. Cold Reg Sci Technol 24:1–6

Tison JL, Brabant F, Dumont I, Stefels J (2010) High resolution DMS and DMSP time series profiles in decaying summer first-year sea ice at ISPOL (Western Weddell Sea, Antarctica). J Geophys Res 115:G04044

Trevena AJ, Jones GB, Wright SW, Van den Enden RL (2000) Profiles of DMSP, algal pigments, nutrients, and salinity in pack ice from eastern Antarctica. J Sea Res 43:265–273

Trimborn S, Hoppe CJM, Taylor BB, Bracher A, Hassler C (2015) Physiological characteristics of open ocean and coastal phytoplankton communities of Western Antarctic Peninsula and Drake Passage waters. Deep Sea Res I 98:115–124

Turner J, Colwell SR, Marshall GJ, Lachlan-Cope TA and others (2005) Antarctic climate change during the last 50 years. Int J Climatol 25:279–294

Van de Poll WH, Lagunas M, de Vries T, Visser RJW, Buma AGJ (2011) Non-photochemical quenching of chlorophyll fluorescence and xanthophyll cycle responses after excess PAR and UVR in *Chaetoceros brevis, Phaeocystis antarctica* and coastal Antarctic phytoplankton. Mar Ecol Prog Ser 426:119–131

Van Heukelem L, Thomas CS (2001) Computer-assisted high performance liquid chromatography method development with applications to the isolation and analysis of phytoplankton pigments. J Chromatogr A 910:31–49

Van Leeuwe MA, Stefels J (1998) Effects of iron and light stress on the biochemical composition of Antarctic *Phaeocystis* sp. (Prymnesiophyceae). II. Pigment composition. J Phycol 34:496–503

Van Leeuwe MA, Stefels J (2007) Photosynthetic responses in *Phaeocystis antarctica* towards varying light and iron conditions. Biogeochemistry 83:61–70

Vancoppenolle M, Meiners KM, Michel C, Bopp L and others (2013) Role of sea ice in global biogeochemical cycles: emerging views and challenges. Quat Sci Rev 79:207–230

Varela M, Fernandez E, Serret P (2002) Size-fractionated phytoplankton biomass and primary production in the

Gerlache and south Bransfield Straits (Antarctic Peninsula) in Austral summer 1995–1996. Deep Sea Res II 49:749–768

Vaughan DG, Marshall GJ, Connolley WM, Parkinson C, Mulvaney R, Hodgson DA, King JC (2003) Recent rapid regional climate warming on the Antarctic Peninsula. Clim Change 60:243–274

Venables HJ, Clarke A, Meredith MP (2013) Wintertime controls on summer stratification and productivity at the western Antarctic Peninsula. Limnol Oceanogr 58: 1035–1047

Vernet M, Martinson D, Iannuzzi R, Stammerjohn S and others (2008) Primary production within the sea-ice zone west of the Antarctic Peninsula. I. Sea ice, summer mixed layer, and irradiance. Deep Sea Res II 55:2068–2085

Wadhams P, Lange MA, Ackley SF (1987) The ice thickness distribution across the Atlantic sector of the Antarctic Ocean in midwinter. J Geophys Res 92:14535–14552

Waite A, Fisher A, Thompson PA, Harrison PJ (1997) Sinking rate versus cell volume relationships illuminate sinking rate control mechanisms in marine diatoms. Mar Ecol Prog Ser 157:97–108

Appendix. Additional data for the evaluation of HPLC and FlowCam methods in assessing community composition of ice algal communities

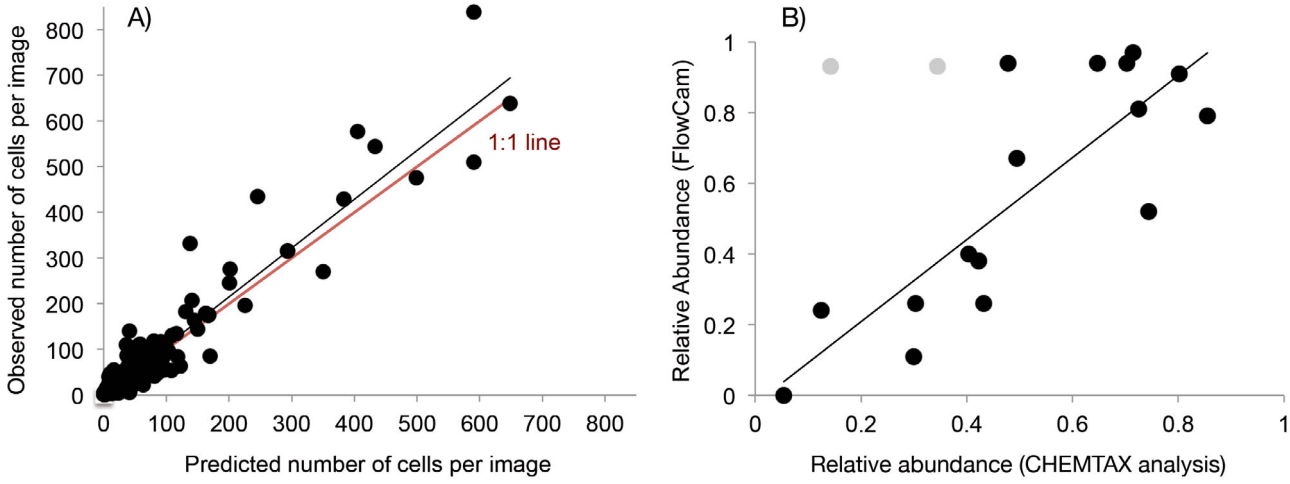

Fig. A1. Evaluation of methods to calculate relative abundance of *Phaeocystis antarctica* in ice algal communities. (A) Predicted versus observed *P. antarctica* cells in FlowCam test data set ($y = 1.07x + 1.41$, $R^2 = 0.91$, $p < 0.001$). (B) Agreement between relative abundance estimates from FlowCam analysis and CHEMTAX analysis for *P. antarctica* (black circles, outliers in gray; $y = 1.16x - 0.02$, $R^2 = 0.69$)

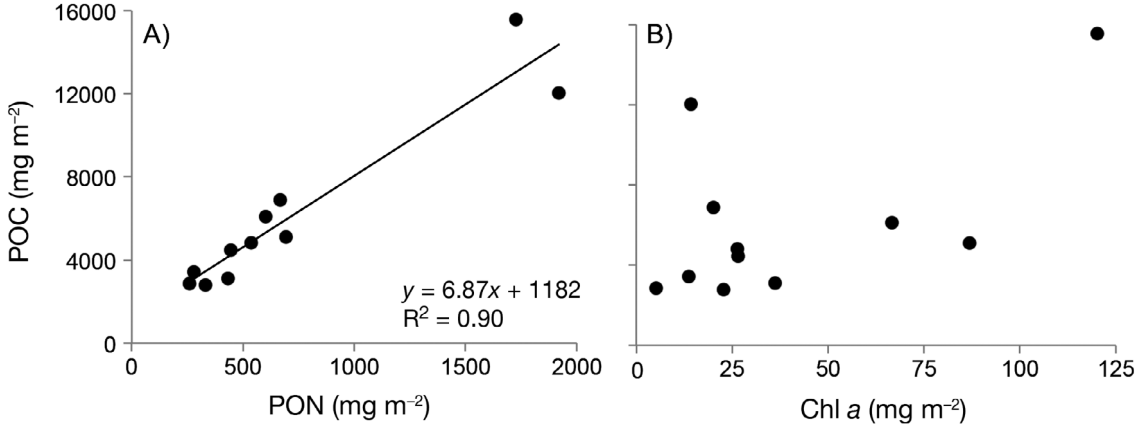

Fig. A2. Relationship between different proxies for biomass in sea ice (mg m^{-2}): (A) particulate organic carbon (POC) versus particulate organic nitrogen (PON) and (B) POC versus chl *a*

Table A1. Initial and final pigment ratios for CHEMTAX-HPLC analysis of ice algal communities in slush and non-slush layers. Per: peridinin, 19-But: 19-butanoyloxyfucoxanthin, 19-Hex: 19-hexanoyloxyfucoxanthin, Fuco: fucoxanthin, Allo: alloxanthin, Viola: violaxanthin

	Algal pigments							
	Per	19-But	Fuco	19-Hex	Chl c_3	Allo	Viola	Chl *b*
Initial								
Prasinophytes	0.00	0.00	0.00	0.00	0.00	0.00	0.03	0.72
Dinoflagellates	0.69	0.00	0.00	0.00	0.00	0.00	0.00	0.00
Cryptophytes	0.00	0.00	0.00	0.00	0.00	0.31	0.00	0.00
Haptophytes 1	0.00	0.05	0.23	0.65	0.10	0.00	0.00	0.00
Pelagophytes	0.00	0.20	0.15	0.25	0.10	0.00	0.00	0.00
Diatoms	0.00	0.00	0.56	0.00	0.00	0.00	0.00	0.00
Final (non-slush)[a]								
Prasinophytes	0.00	0.00	0.00	0.00	0.00	0.00	0.03	0.72
Dinoflagellates	0.69	0.00	0.00	0.00	0.00	0.00	0.00	0.00
Cryptophytes	0.00	0.00	0.00	0.00	0.00	0.31	0.00	0.00
Haptophytes 1	0.00	0.01	0.24	0.53	0.18	0.00	0.00	0.00
Pelagophytes	0.00	0.20	0.15	0.25	0.03	0.00	0.00	0.00
Diatoms	0.00	0.00	0.68	0.00	0.00	0.00	0.00	0.00
Final (slush)[b]								
Prasinophytes	0.00	0.00	0.00	0.00	0.00	0.00	0.03	0.72
Dinoflagellates	0.69	0.00	0.00	0.00	0.00	0.00	0.00	0.00
Cryptophytes	0.00	0.00	0.00	0.00	0.00	0.31	0.00	0.00
Haptophytes 1	0.00	0.01	0.23	0.52	0.18	0.00	0.00	0.00
Pelagophytes	0.00	0.20	0.15	0.25	0.14	0.00	0.00	0.00
Diatoms	0.00	0.00	0.65	0.00	0.00	0.00	0.00	0.00

[a]RMS error = 0.051
[b]RMS error = 0.103

Editorial responsibility: Steven Lohrenz, New Bedford, Massachusetts, USA

Submitted: May 4, 2017; Accepted: October 2, 2017
Proofs received from author(s): December 15, 2017